March 29th, 2019

CFM presentation
Fan blades fragments trajectories and Philadelphia inlet damage assessment

Table of Contents

List of Figures

Figure **Title** **Page**

List of Tables

Table **Title** **Page**

Section 1.0 Summary

The objective of this report is to document the CFM assessment of fan blade fragments trajectories and Philadelphia inlet damage presented to the investigative parties during the meeting held March 5-6, 2019 in Cincinnati, Ohio.

Regarding fan blade fragmentation, CFM described that based on recovered fragments (one mid span fragment and the root fragment) and three/four witness marks identified on fan case, one tip fragment and two/three mid span fragments have exited forward. This fragmentation and direction of the fragments are very similar to what was observed during FBO certification test 874002/2 performed with Boeing type design inlet.

As shared during certification process, Tip Fragment is the highest energy fragment. Based on CFM data on tip and mid span fragments mass and velocity, CFM has estimated the average value of total mid span fragments kinetic energy to be 60% lower than tip fragment kinetic energy. The maximum energy of an individual mid span fragment will be less**.**

With respect to the Tip fragment trajectory, based on certification engine test 874 002/2 and Engineering Rig test 4, both performed with Boeing inlets, data supports a continuous tip fragment trajectory aft and forward of A1 flange. Tip fragment edge imprints are observed on fan case when crossing A1 flange with an angle of 15°. Because trajectory of Tip fragment is continuous aft and forward of A1 flange, Tip fragment CG trajectory is assumed to cross A1 flange with a 15° angle in both cases.

For the Philadelphia event, it has been identified that although tip fragment edge crosses A1 flange with an angle of 15° based on imprints on fan case between 6:00 and 7:00, the tip fragment CG has probably crossed A1 flange with a maximum angle of 20°. This angle is supported by physical data: three distinct Tip fragment trailing edge imprints on the Fan case corresponding to three locations of the tip fragment when exiting the fan case. Those imprints indicate a tip fragment rotational motion. In addition, no continuous tip fragment trajectory is observed in inlet diameter post A1 flange. However, damage, consisting of missing material, is observed on inlet A1 flange lip which explains the lack of tip fragment markings forward of the A1 flange. A potential scenario is when the Tip fragment enters the inlet, it impacts the inlet A1 flange lip, shears the corner resulting in a “divot”. The tip fragment then loses contact with the inlet in this area as a result of the corner impact. Analysis supports that the tip fragment impact with A1 flange aft facing step results in more forward fragment trajectory in the inlet and increased fragment energy forward in inlet.

Regarding mid span fragments, two/three witness marks have been identified which are likely due to blade mid span fragments: one/two crossing A1 flange at 7:00 with angles of 31-34° and one crossing A1 flange at 7:35 with an angle of 19°.

Based on CFM fragments trajectory analysis and inlet damage evidence, CFM has performed additional analysis of the inlet damage Phases (1,2,3) identified during October Structures Group meeting in San Diego.
These initial damage assessments did not fully include the trajectories of the fan blade fragments and the evidence of fragments being present in the area of damage (or not).

This additional analysis supports the inner barrel back skin damage in the Phase 1 area from 10:30 to 11:30 (30 degrees) is likely due to fan blade fragment penetration. This damage was most likely caused by the tip fragment, with one mid span fragment subsequently passing through the penetration area. This behavior is very similar to the certification and development experience, with the exception of the increased forward travel of the tip fragment which could be explained by the divot observed on the inlet A1 flange and the maximum 20° CG trajectory crossing A1 flange as described above. Based on the evidence, those fragments have also likely penetrated the outer barrel.
The additional inner barrel back skin damages in the Phase 1 area from 11:30 to 12:45 is likely not due to fan blade fragment penetration based on lack of radial outward deformation of the

backskin, lack of honeycomb core radial crushing, a lack of fragment trajectory evidence in this area, and no evidence of instantaneous propagation adjacent to fragment penetration. Damage in this area is likely due to subsequent damage propagation due to applied inlet loads.

The inner barrel back skin damage in the Phase 2 area from 7:30 to 8:30 is likely not due to fan blade fragment penetration based on a lack of radial outward deformation of the backskin, lack of honeycomb core radial crushing, a lack of fragment trajectory evidence in this area. Also at 7:30, some titanium particles have been found. CFM analysis shows intact septum above the honeycomb cut where this particle was found. It is not physically possible that a primary blade fragment could have made the cut in the honeycomb without first cutting the septum. This indicates that the Ti 6-4 material found in the honeycomb at 7:30 position must have come from a source other than a primary blade fragment. CFM substantiates other potential sources for titanium particles including small low energy fan blades fragments and the inlet forward bulkhead which could have impacted the surface after the inlet separated.

The inner barrel back skin damage in the Phase 3 area from 5:00 to 7:30 and 9:00 to 10:30 is likely not due to fan blade fragment penetration. There is no evidence of radial outward deformation of the backskin, no honeycomb core radial crushing, and there is no evidence of primary fragment marks or trajectories aligned with the Phase 3 from 5:00 to 7:30 damage zone on the perf skin on either the attach ring or D duct side of the inner barrel separation.

Additional analysis of the inlet inner barrel honeycomb attached to the 9:00 inner barrel splice or beam has also been made. This area was of interest because initial Party assessments suggested that the tip fragment contacted this area and crushed the honeycomb in a circumferential direction. The splice plate at 9:00 is bent backwards around the outside of the inner barrel. This is believed to be a result of impact with the separated, forward part of the inlet departing in an aircraft outward direction (towards wing tip). Significant loads must have been imparted to the splice plate to deform this stiff, structural element. Trajectory angles required to impact the honeycomb in this area are approximately 40 degrees which is not consistent with any tip trajectory evidence (witness marks), the direction of honeycomb crushing (circumferential), the consistent, prior experience of rig and engine testing or LS-Dyna tip trajectory predictions. In addition, the axial width of the crushed honeycomb is wider than the expected width of a fragment.

In conclusion:

- **In Philadelphia event, fan blade fragmentation and direction of the fragments are very similar to what was observed during FBO certification test 874002/2.**
- **Three/four fan blades fragments have come forward of A1 flange based on witness marks: one tip fragment and two/three mid span fragments.**
- **Tip fragment CG has crossed A1 flange with a maximum angle of 20° compared to the 15° experienced during FBO certification test 874002/2.**
- **Presence of damage at the inlet lip where tip fragment crosses A1 flange supports that the tip fragment impacted an aft facing step at the inlet A1 flange. This was not experienced during certification test. Also there is no continuous witness mark from tip fragment forward of A1 flange as observed in the certification test. This could result in tip fragment trajectory variation in the inlet.**
- **CFM inlet damage analysis supports the inner barrel back skin damage from primary blade fragment penetration is limited to 30 degrees (10:30 to 11:30). Data does not support that fan blade fragment created damage beyond 30 degrees to the inner barrel back skin.**

Section 2.0 Fan Blade fragmentation

2.1 Fan Blade fragmentation: certification experience and events

During a Fan Blade out event, after fan blade is released, the fan blade hits the fan case and is fragmented into several pieces: tip fragment, mid –span fragments and root fragment. CFM test and field experience can be summarized as follows: the Tip fragment has always gone forward. Mid span fragments have gone both forward and aft. The Root fragment has always gone aft except for Pensacola event where the root fragment went forward during the event based on witness marks.

Figure 2-1 below depicts the CFM56-7B Fan Blade fragmentation experience for the two certification tests and the Pensacola and Philadelphia events with an indication of the direction of the fragments (forward or backward). For the Pensacola event, no fragments were found inside the engine so it is assumed all fragments have gone forward. For the Philadelphia event, assumptions for Fan Blade fragmentation are detailed in the Powerplant Group Chairman's factual report (NTSB DCA18MA142). CFM has described, based on recovered fragments (one mid span fragment and the root fragment) and witness marks on Fan case, that there must have been one tip fragment and two/three mid fragments that have exited forward. This fragmentation and direction of the fragments is very similar to what was observed during FBO certification test 874002/2 performed with Boeing type design inlet.

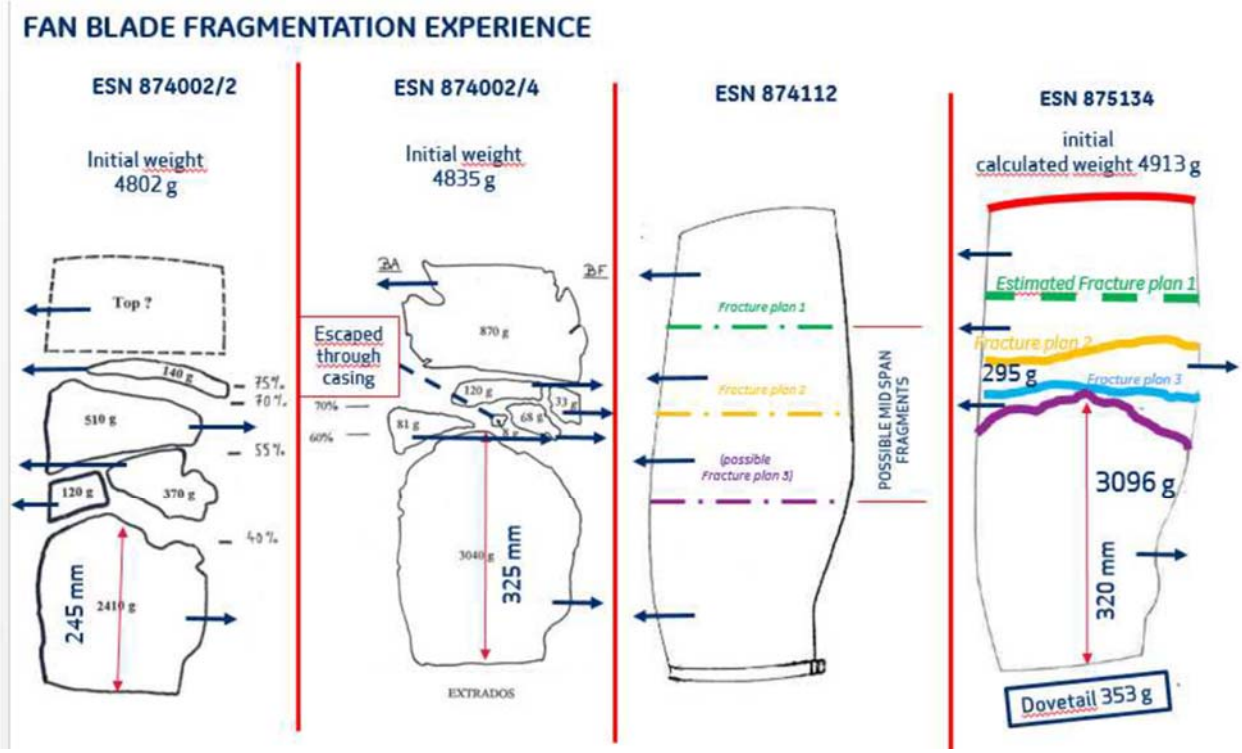

Figure 2-1 : CFM56-7B fan blade fragmentation – Certification experience versus Pensacola and Philadelphia events

2.2 Fan blade fragment energy assessment

Objective of this paragraph is to estimate fragment energies for the Philadelphia event. Fan Blade kinetic energy is calculated as follows:

$$E = \frac{1}{2} M V^2$$

Where E = Fragment kinetic energy

M = Fragment mass

V = Fragment velocity

Fragments mass assessment

Based on total mass of the blade and fragments recovered inside engine, maximum 2.6 lbs fragments went forward in Philadelphia event (some small fragments could have gone backward and been ingested).

Tip fragment mass is unknown but based on experience on certification and rig tests CFM can assume it was between 1.26 lbs and 1.9 lbs. Total mid span fragment mass, based on experience, is estimated to be between 0.65 and 1.3 lbs.

Fragments velocity assessment

Tip fragment velocity is based on CFM56-7B Fan Blade Out rig tests and engine certification tests experience performed at redline speed (> Philadelphia event speed). It was measured from high-speed camera films. Min and max values were 594ft/s and 791 ft/s. Note for Tip fragment velocity, LS-DYNA predicts slightly higher velocity than velocity measured from films (max calculated speed is 853 ft/s).

Mid span fragments velocity has been calculated with LS-DYNA including sensitivity studies which gives a range from 525ft/s to 591 ft/s.

The range for tip fragment and total mid span fragments kinetic energies are shared in table 2-1 and 2-2.

	Tip fragment				
	Mass (measured)		**Velocity (measured)**		**Kinetic energy**
	lbs	Kg	ft/s	m/s	**KJ**
Avg	1,58	0,72	693	211	**16**
Min	1,26	0,57	594	181	**9,4**
Max	1,9	0,86	791	241	**25**

Table 2-1 : Tip fragment exiting the fan case kinetic energy

Note:

Tip fragment assessed kinetic energy is consistent with mass and velocities provided to Boeing during CFM56-7B engine development (cf. ECM N° 8604 Feb 7, 1997): 2lbs and 880 ft/s which results in a kinetic energy of 32 KJ.

	Mid fragments				
	Mass (measured)		Velocity (calculated)		Kinetic energy
	lbs	Kg	ft/s	m/s	**KJ**
Avg	0,975	0,44	558	170	**6,4**
Min	0,65	0,29	525	160	**3,8**
Max	1,3	0,59	591	180	**9,6**

Table 2-2 : Mid fragments exiting the fan case kinetic energy

Note:

This is total combined mass and energy of all mid span fragments. The maximum energy of an individual mid span fragment will be lower.

Conclusion:

Average span fragment kinetic energy is 60% lower than average Tip fragment kinetic energy.

Section 3.0 Tip fragment trajectory for FBO Rig test 4 and certification test 874-002/2

3.1 Tip fragment trajectory during Engineering FBO test: Rig 4

Engineering FBO test Rig 4 was performed using preliminary Boeing inlet design. During this test, tip fragment penetrated inner barrel back skin at 6 o'clock (~180° from blade release position) and exited through the inlet which had no containment doubler at that time.

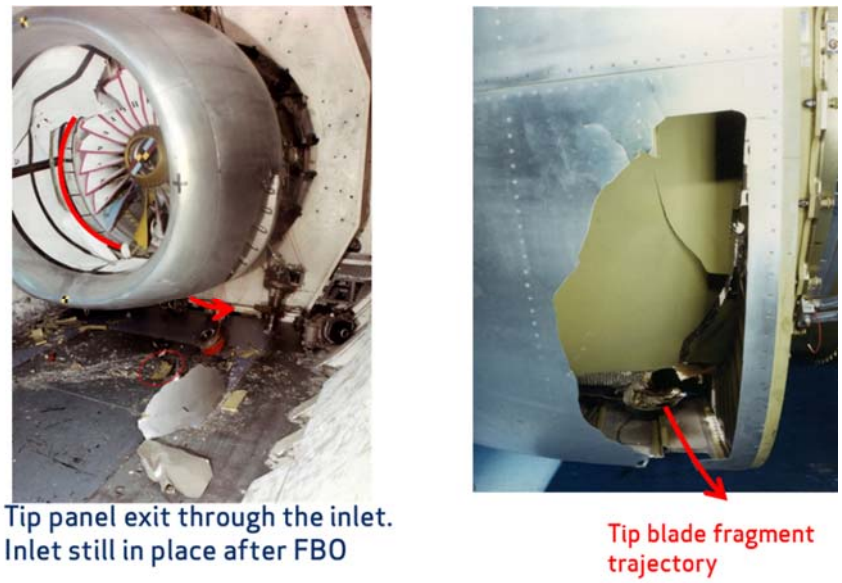

Figure 3-1 : Photographs of engine post FBO RIG test 4 – Tip blade fragment trajectory

Review of photographs of Rig Test 4 shows continuous tip fragment trajectory aft and forward of A1 flange between 2 o'clock and 4 o'clock. Tip fragment edge crossed A1 flange with an angle of 15°. Continuous marks observed on fan case and inlet suggest that fragment center of gravity (CG) had same trajectory as tip fragment edge.

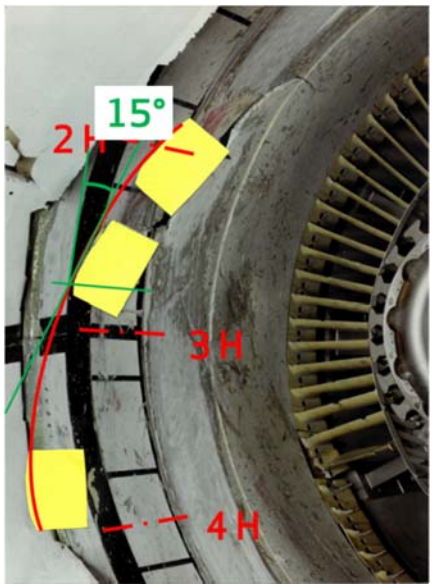

Figure 3-2 : FBO Rig Test 4 - Tip blade fragment trajectory

3.2 CFM56 -7B FBO certification test - engine 874002/2: Tip trajectory

The FBO FAR33 Certification test was performed on CFM56-7B engine 874002/2 including type design Boeing Inlet.

After the FBO certification engine test, the tip fragment marks on the fan case leading up to A1 flange and in the aft inner diameter of the Inlet are visible on the photograph from the test between 1H30 and 3H30 (Clockwise Aft Looking Forward comprising a 60° angle).

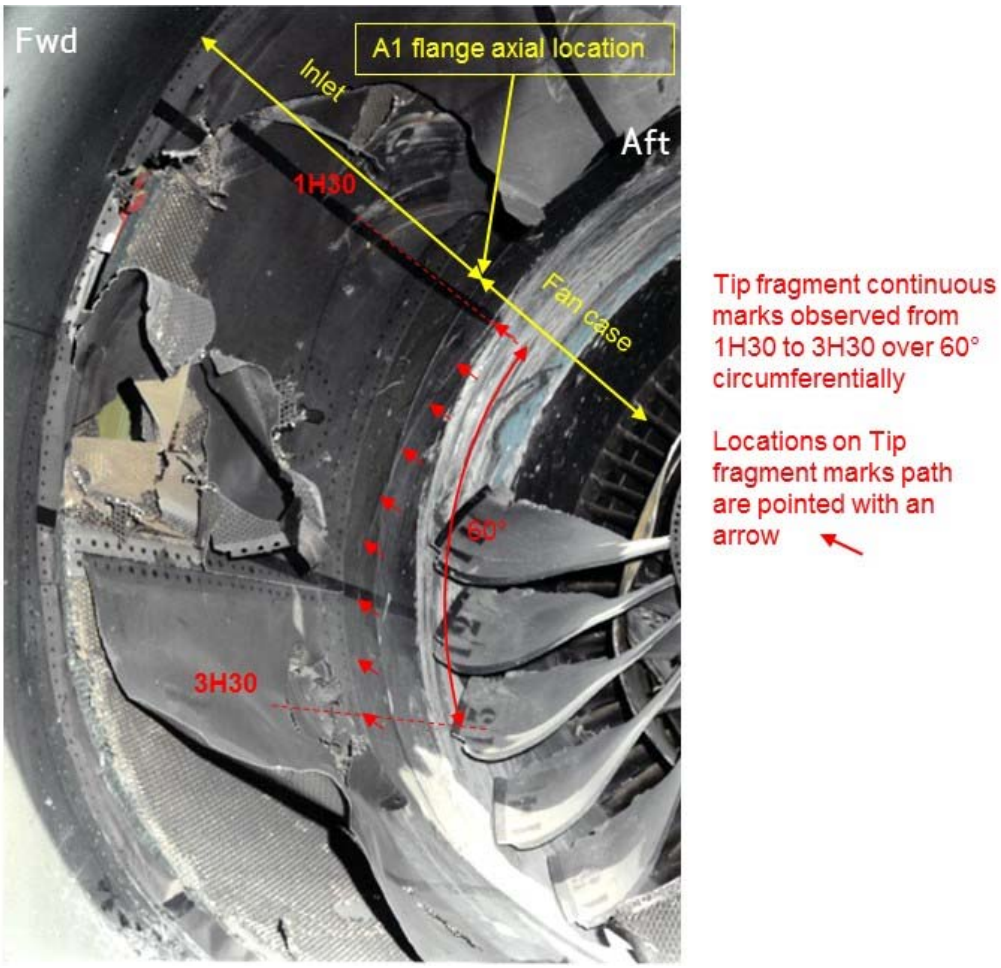

Figure 3-3 : Engine 2/2 front view after FBO Certification test

Those Tip fragment marks are made by the edge of the tip fragment and provide information on its trajectory. The position of those marks relative to A1 flange plane has been measured as illustrated in Figure 3-4.

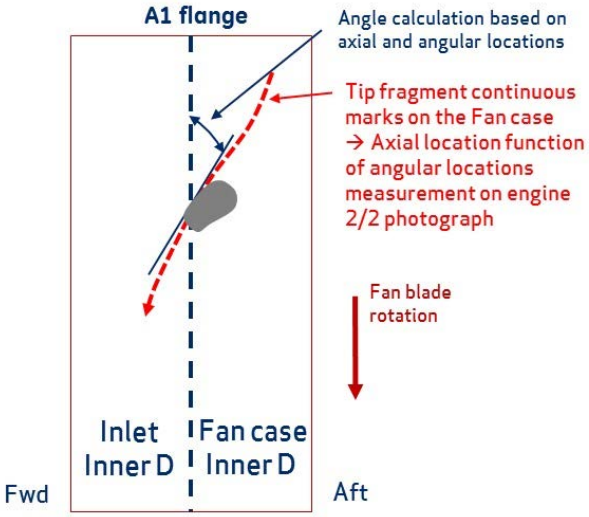

Figure 3-4 : Tip fragment marks on Fan case and Inlet inner Diameter observed around A1 flange

The axial and angular locations measurements of the 9 points observed on the continuous Tip fragment marks are summarized in Table 3-1.

Associated angles with A1 flange plane are calculated as follows
Angle at location **i** = Angle of linear trajectory between location **i-1** and location **i**

Tip Fragment marks measurement : Engine 2/2 FBO Certification test				Calculated angle with A1 flange (°)
	Angular location (°)	Curvinilear abscisse (mm)	Distance to A1 Flange (mm)	
Location 1	45	611	-83	
location 2	52,5	713	-68	8
Location 3	60	815	-44	13
Location 4	67,5	917	-16	15
Location 5	75	1019	11	15
Location 6	82,5	1120	31	11
Location 7	90	1222	48	10
Location 8	97,5	1324	69	11
Location 9	105	1426	94	14

Table 3-1 : Tip fragment marks angular and axial measured locations and associated angles

The measured tip fragment marks positions allow to establish the tip fragment edge trajectory as shown in Figure 3-5.

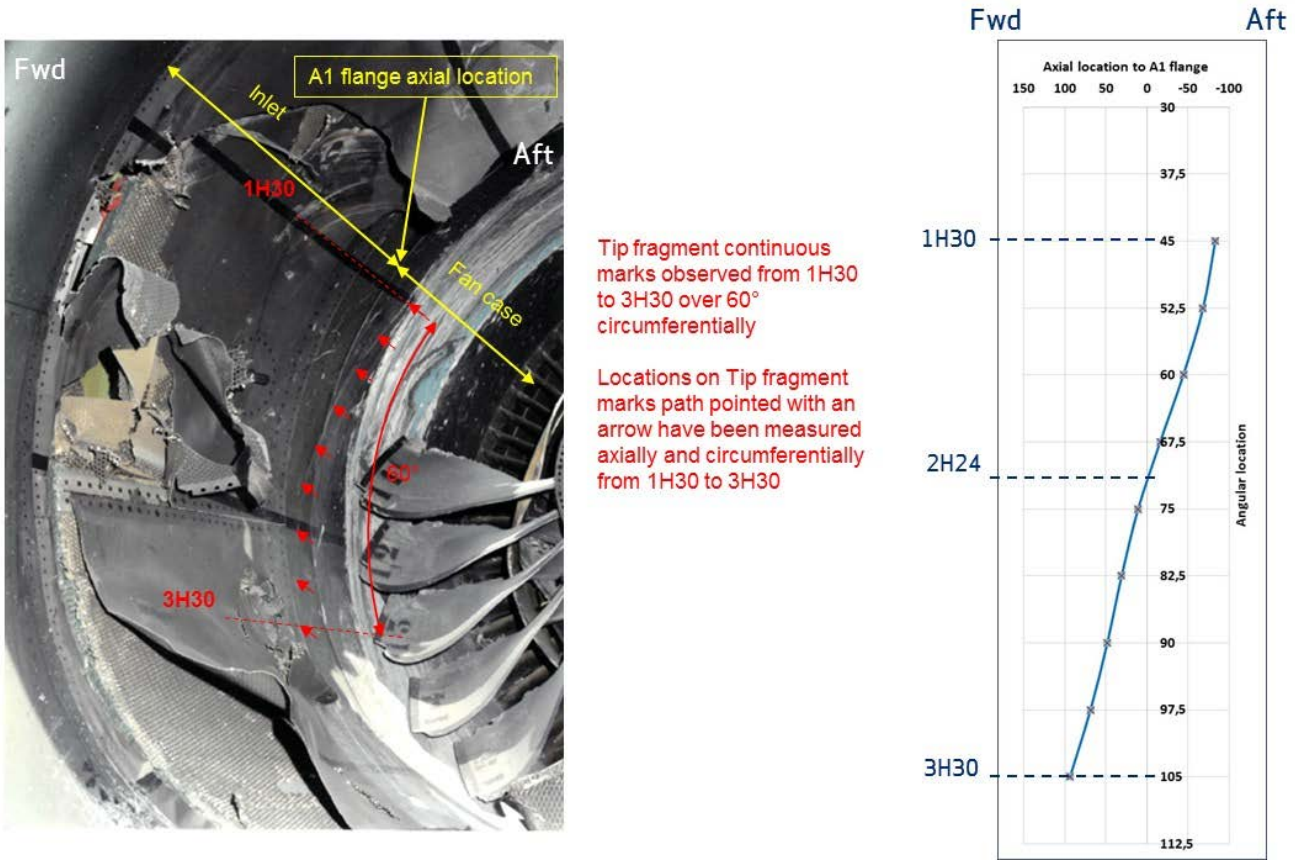

Figure 3-5 : Tip fragment trajectory measured on engine 2/2 around A1 flange

The measured Tip fragment edge marks between1:30 and 3:30 show a nearly rectilinear trajectory, as presented in figure 3-5, with limited variations of the calculated angle with A1 flange plane between 10° and 15°.
From location 2 to location 9 at the end of the marks the average angle is 13°.
The calculated angle when crossing A1 flange is ~15°.

Based on continuous mark from tip fragment observed on Figure 3-5, there is no evidence of Tip fragment tumbling between 1:30 and 3:30.
Moreover, on the engine 2/2 high speed films, no Tip fragment tumbling is observed between 3:00 and 4:00 on engine 2/2. Earlier than the 3:00 clock position, the Tip fragment cannot be observed on high speed films) as presented in figure 3-6. Only Tip fragment wobbling (not tumbling) is observed.

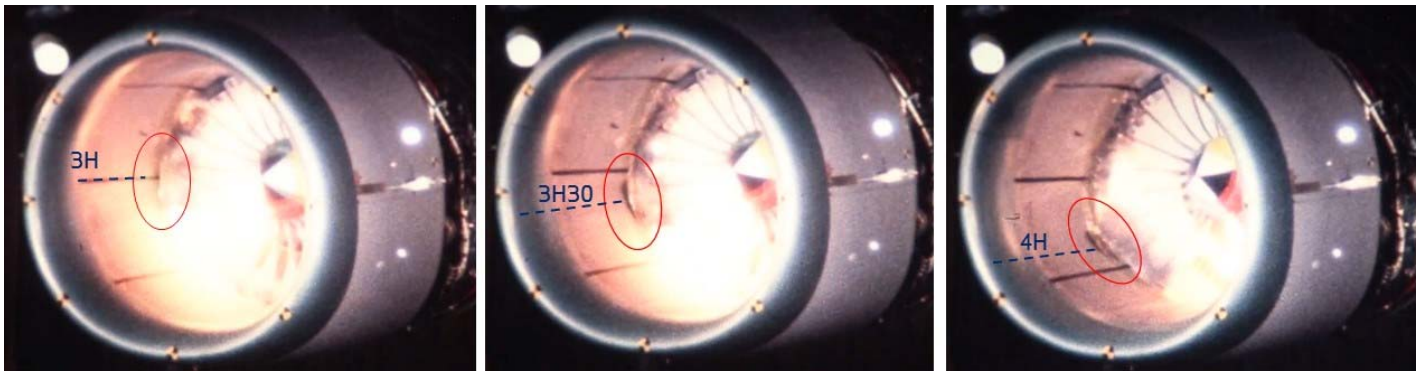

Figure 3-6 : Tip fragment sliding between 3:00 and 4:00

The witness marks and corresponding tip fragment trajectory for engine 874-002/2 can be summarized as follows:

Tip fragment edge marks measurement and associated angles Fan case and Inlet inner Diameter around A1 flange show a nearly rectilinear trajectory of the tip fragment edge:

- With limited angle variations between 10° and 15 with an average angle of ~13°
- ~15° angle when crossing A1 flange

As the trajectory of the Tip fragment edge is continuous and nearly rectilinear, likely with Tip fragment wobbling and no evidence of Tip fragment tumbling, the trajectory of the tip fragment CG will be very similar to the Tip fragment edge trajectory and the associated angles are predicted to be between 10° and 15°.

Note:

Tip fragment CG trajectory is not directly observable on engine 2/2 Fan case and around A1 flange, only Tip fragment *edge trajectory* marks can be observed.
The Tip fragment CG trajectory will be very similar to the Tip fragment edge trajectory but with an angular shift due to the Tip fragment dimensions.

3.3 LS-DYNA prediction for engine 2/2 FBO conditions

LS-DYNA analysis of engine 2/2 FBO Certification test conditions have been performed and shows a high level of correlation up to half a revolution (5.5ms) with engine 2/2 FBO Certification measurements. The Boeing Inlet model received as of 2018 September 3rd has been used in the analysis.

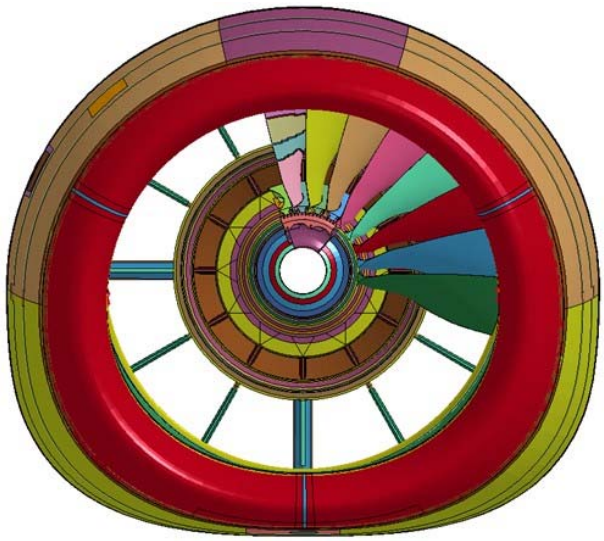

Figure 3-7 : CFM56-7B engine 2/2 LS-DYNA model

3.3.1 LS-DYNA calculation results

The results of LS-DYNA analysis are described on Figure 3-8.

- The Tip fragment CG predicted trajectory is analyzed from the blade release angle up to half a revolution
- The Tip fragment CG crosses A1 flange at 5.3ms around 4:15 before half a revolution (5.5ms)

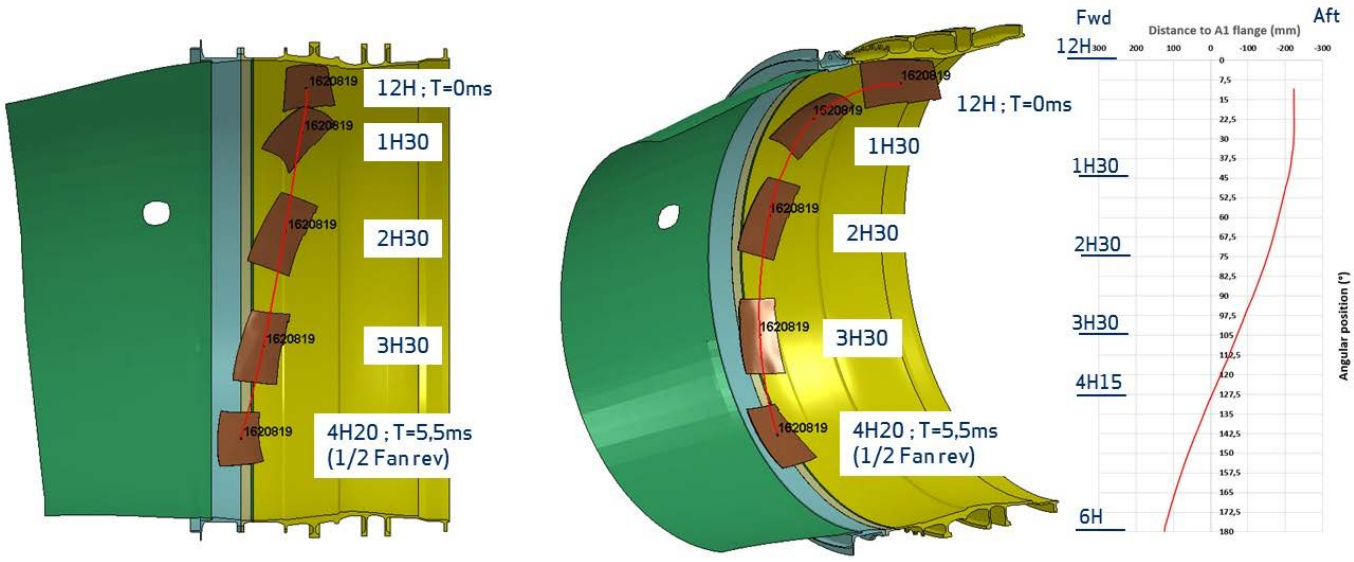

Figure 3-8 : LS-DYNA calculated Tip fragment CG trajectory for engine 2/2 Certification test conditions

Tip fragment CG trajectory and associated angle with A1 flange are described on Figure 3-9

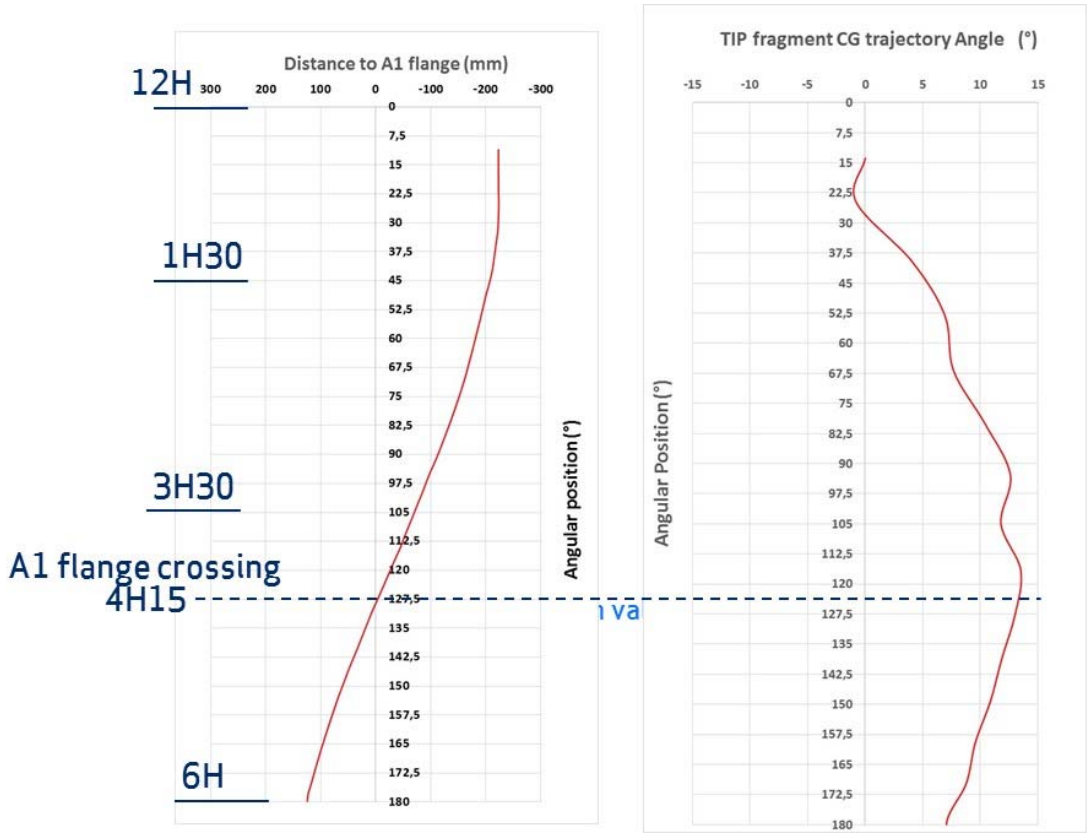

Figure 3-9 : LS-DYNA calculated Tip fragment CG trajectory for engine 2/2 Certification test conditions

The calculated Tip fragment CG trajectory angle when crossing A1 flange is 13.2°

Additional sensitivity studies of LS-DYNA parameters including friction coefficient variation) have been performed and show similar results for the Tip fragment CG trajectory angle at A1 Flange crossing with results falling between 10° and 16.5°.

3.3.2 Comparison with FBO certification test engine 874-002/2

Objective is to superimpose tip fragment edge marks on engine 874-002/2 (Figure 3-5) and tip fragment CG trajectory calculated by LS-DYNA (Figure 3-9) for trajectory angle comparison.

Details of the comparison process:

- The measured Tip fragment edge marks cross A1 flange at 2:24 on engine 874-002/2

- Tip fragment CG crossing A1 flange on engine 874-002/2:

  As explained in section 3.3.1, Tip fragment CG trajectory will be very similar to the Tip fragment edge trajectory but the angular location of the Tip fragment CG will be shifted from the Tip fragment edge due to Tip fragment dimensions. The Tip fragment CG trajectory crosses A1 flange around 3:30 based on test evidence.

- In LS-DYNA calculation, Tip fragment CG trajectory crosses A1 flange at 4:15

- In the following figure 3-10, both Tip fragment CG trajectory assessed on engine 874-002/2 and LS-DYNA calculated CG trajectory are superimposed considering identical A1 flange crossing angular location at 4:15 to compare their trajectory angles.

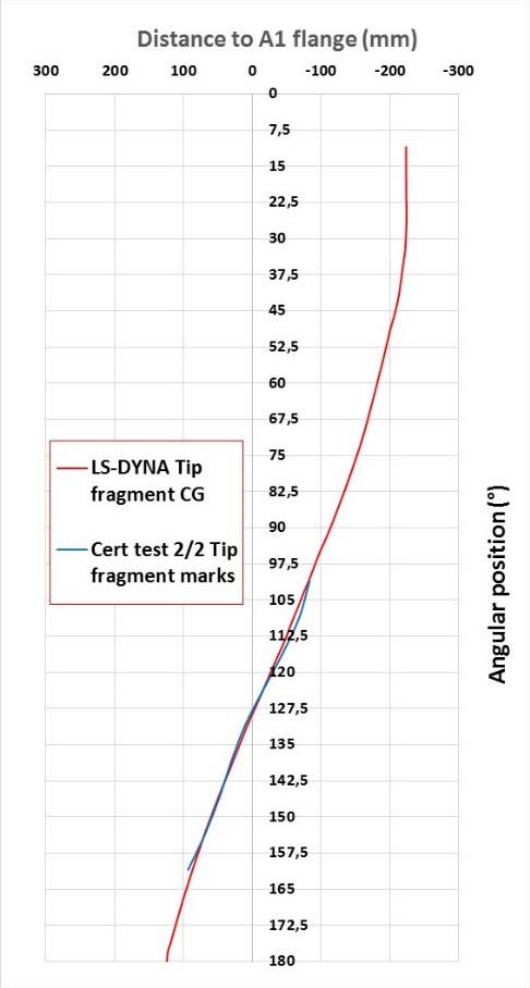

Figure 3-10 : Engine 2/2 Tip fragment marks and LS-DYNA Tip fragment CG trajectory superimposed

This comparison indicates that the Tip fragment edge marks on engine 874-002/2 (Figure 3-5) and the Tip fragment CG trajectory calculated by LS-DYNA (Figure 3-9) when superimposed (Figure 3-10) show very similar trajectories with following angles at A1 axial plane:

- Calculated Tip fragment CG trajectory angle at A1 Flange crossing is 13.2°.

- Assessed Tip fragment CG trajectory on engine 2/2 show a 15° angle at A1 flange crossing, and angle variations along the trajectory between 10° and 15

3.3.3 Conclusion

LS-DYNA predicted Tip fragment CG trajectory and angle at A1 Flange crossing are consistent with Tip fragment CG trajectory and angle at A1 Flange estimated from engine 2/2 visual evidence.

3.4 Conclusion: Tip fragment trajectory based on Rig 4 and certification test 2/2

Tip fragment edge marks on Rig 4 and engine 2/2 Fan cases and Inlet inner Diameter around A1 flange show a nearly rectilinear trajectory of the tip fragment.

- Measurements based on photographs from Rig 4 and cert test 874-002/2 show a 15° angle when crossing A1 flange
- On cert test 874-002/2, the trajectory forward and aft A1 flange shows limited angle variations between 10° and 15° (angle with A1 flange) with an average of 13°.

With respect to the certification test 874-002/2, the trajectory of the Tip fragment edge is continuous and nearly rectilinear. The witness marks and analysis supports potential Tip fragment wobbling with no evidence of Tip fragment tumbling; the trajectory of the tip fragment CG will be very similar to the Tip fragment edge trajectory and the associated angles are predicted to be between 10° and 15°.

Section 4.0 Tip fragment trajectory for Pensacola and Philadelphia events

4.1 Tip fragment imprints on fan case crossing A1 flange

The tip fragment witness marks at A1 flange location on the Fan case show very similar angle ~15° between Pensacola engine 874112, Philadelphia engine 875134 and FBO Certification test engine 874002/2. This is based on *physical evidence*; that is, the tip panel imprints on fan case.

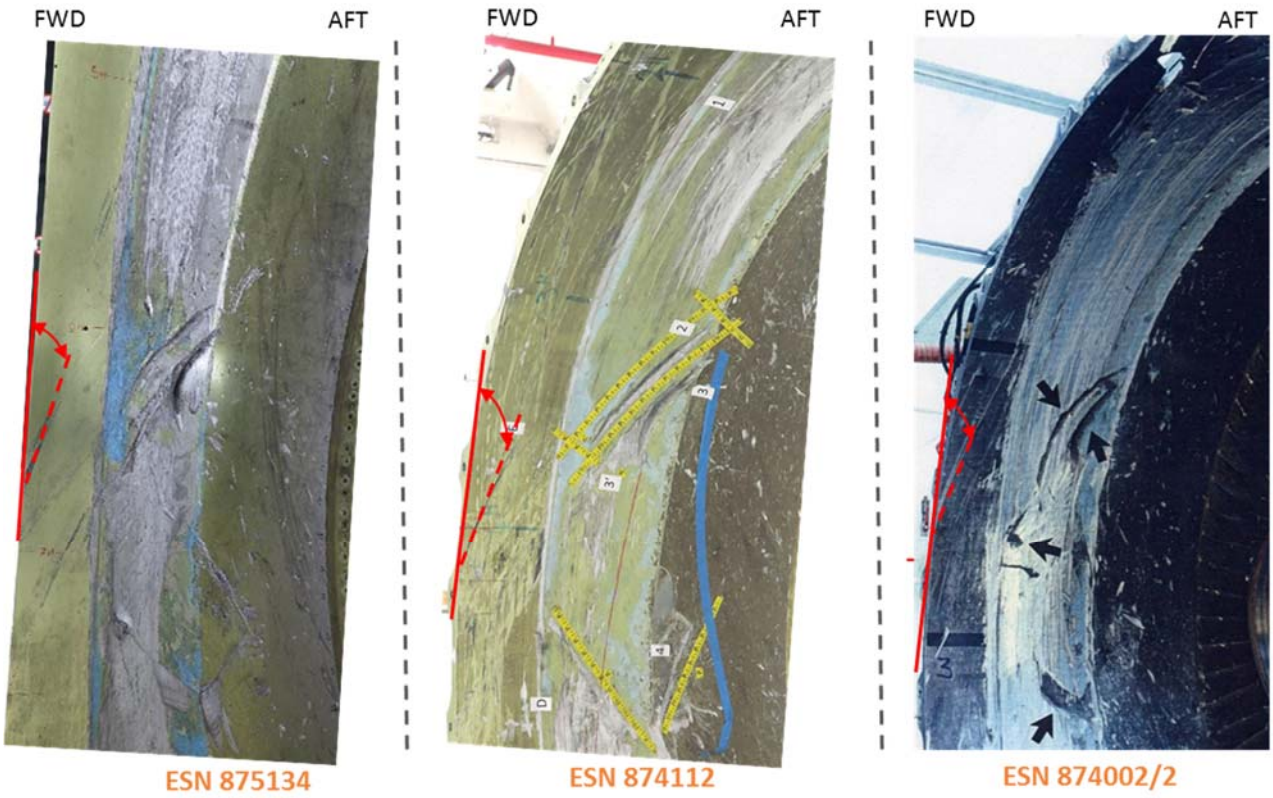

Figure 4-1 : Tip fragment imprints on the Fan case angle at A1 flange

4.1.1 Tip fragment imprints on fan case crossing A1 flange – Pensacola

The angle of tip fragment witness marks on the Fan case at A1 flange location was measured on Pensacola Fan case: the result is ~14° as illustrated on Figure 4-2.

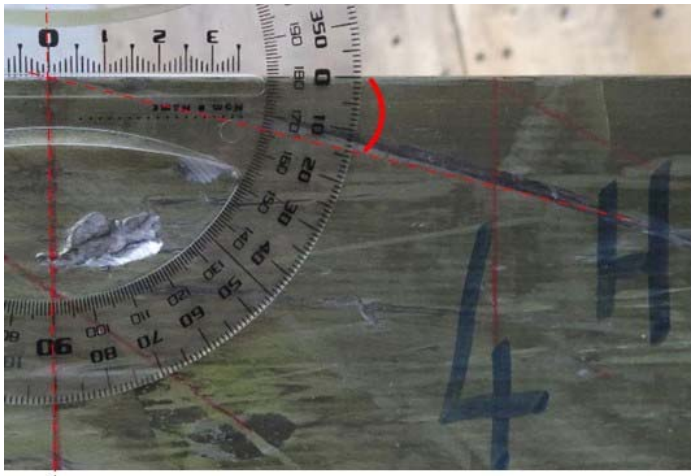

Figure 4-2 : Tip fragment mark on the Fan case measured angle at A1 flange on Pensacola engine 874112 Fan case

4.1.2 Tip fragment imprints on fan case crossing A1 flange – Philadelphia

The angle of last tip fragment mark on the Fan case at A1 flange location was measured on Philadelphia Fan case at 15° as shown in Figure 4-3.

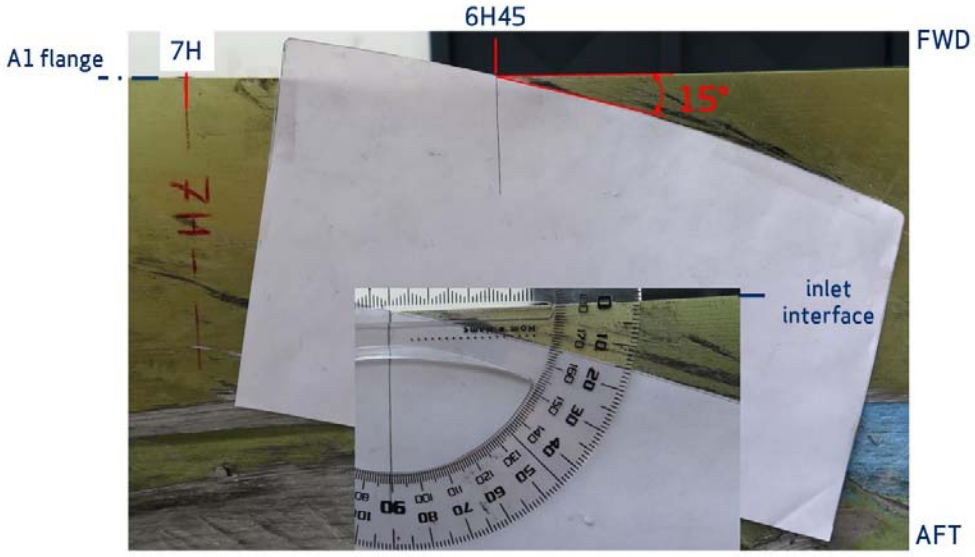

Figure 4-3 : Tip fragment mark on the Fan case and angle measurement at A1 flange on Philadelphia engine 875134 Fan case

The Tip fragment witness marks and measured angles at A1 flange on Pensacola and Philadelphia Fan cases are representative of the angle of Tip fragment *edge* at a particular instant, but the Tip fragment *CG trajectory* can be different.

Therefore, additional analyses were performed to better estimate the trajectory of the Tip fragment CG. These additional analyses are presented in Chapter 4.2 for Pensacola engine and in Chapter 4.3 for the Philadelphia engine.

4.2 Analysis of tip fragment marks on fan case to estimate Tip fragment Center of Gravity trajectory on Pensacola engine 874112

Tip fragment marks on the Fan case are the only data available to estimate the tip fragment edge trajectory up to A1 flange, as no evidence (witness marks) of tip fragment trajectory are observed on the Inlet inner diameter just forward of the A1 flange as shown in Figure 4-4.

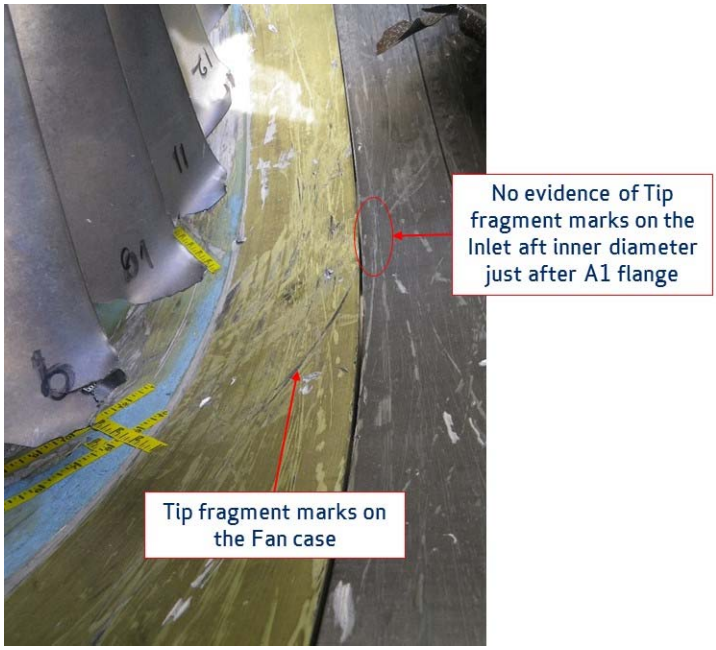

Figure 4-4 : Tip fragment marks observed on Pensacola engine 874112 Fan case

Tip fragment marks are observed between 3:00 and 4:15 on engine 874112 Fan case:

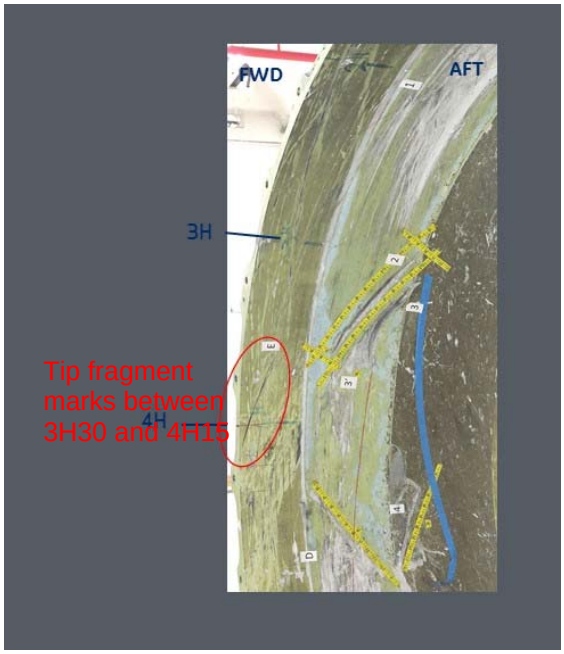

Figure 4-5 : Tip fragment marks measurement on Pensacola engine 874112 Fan case

The detailed analysis of these tip fragment marks on the Fan case shows one local Tip fragment trailing edge imprint on the Fan case, and edge marks.

position	+75 mm	+50mm	0	-50 mm	-100 mm	-150 mm	-215 mm
X	0 mm	6 mm	18 mm	33 mm	53 mm	74 mm	109 mm

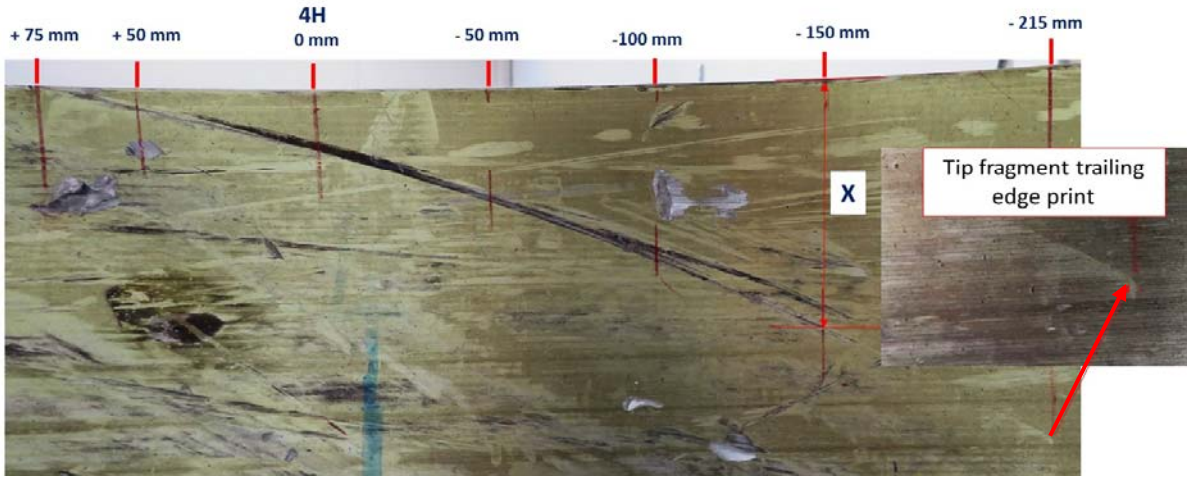

Figure 4-6 : Tip fragment marks measurements on Pensacola engine 874112 Fan case

As described in Figure 4-6, the distance to A1 flange of tip fragment marks has been measured at different circumferential positions. Based on those measurement, the Tip fragment witness mark calculated angle on Pensacola engine 874112 Fan case when crossing A1 flange is 13°.

This value is very similar to the angle of the witness marks at A1 flange (14°) presented in Figure 3-2.

However, due to the limited length of the Tip fragment marks, it is difficult to determine if this trajectory and angle at A1 flange is completely representative of the Tip fragment CG trajectory and angle for Pensacola event.

4.3 Analysis of Tip fragment marks on Fan case to estimate Tip fragment CG trajectory on Philadelphia engine 875134

Tip fragment marks on the Fan case are the only data available to estimate the tip fragment edge trajectory up to A1 flange, as no evidence of tip fragment trajectory is observed on the Inlet inner diameter just forward of the A1 flange.

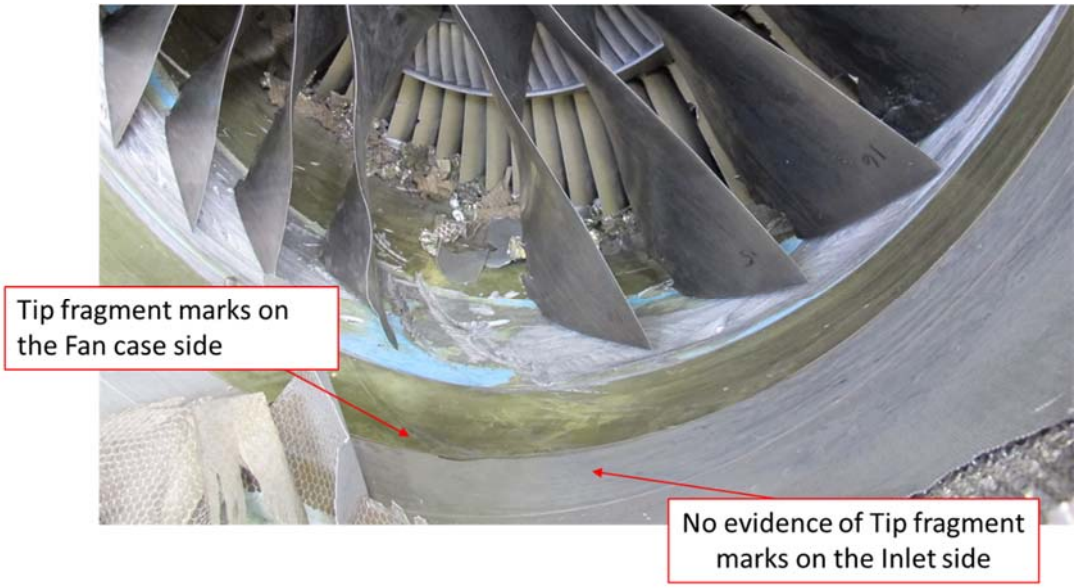

Figure 4-7 : Tip fragment marks on Philadelphia engine 875134

Tip fragments marks are observed between 6:00 and 7:00 on engine 875134 Fan case. See Figure 4-8.

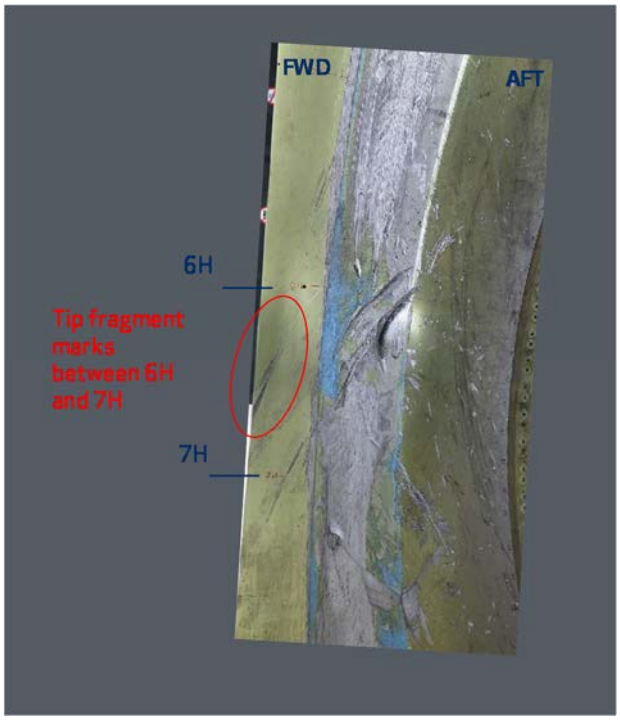

Figure 4-8 : Tip fragment marks on Philadelphia engine 875134 Fan case between 6:00 and 7:00

Detailed analysis of these tip fragment marks on fan case show **three** distinct Tip fragment trailing edge imprints on the Fan case. A photograph of the blade Tip trailing edge radius is shown in Figure 4-9.

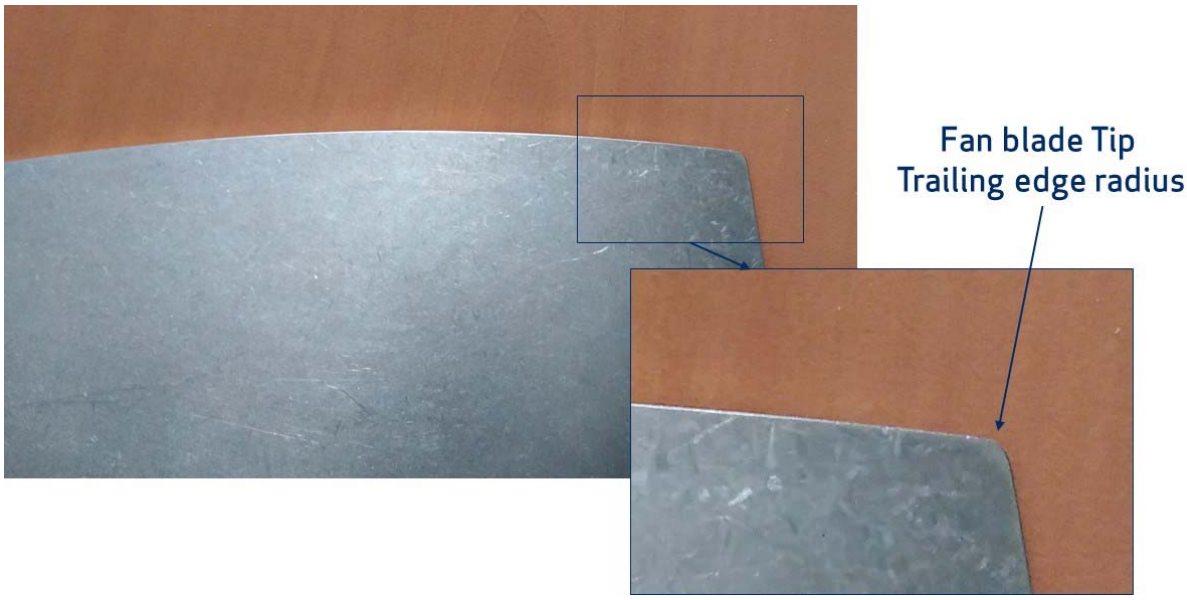

Figure 4-9 : Fan blade Tip trailing edge radius

To estimate Tip fragment center of gravity trajectory, the methodology used is the following:

- Step#1: Each of these three imprints of the Tip fragment trailing edge radius is used to locate precisely the Tip fragment using a typical tip fragment shape. See Figure 4-10.

- Step#2: The corresponding three Tip fragment Center of Gravity locations are used to estimate the trajectory of the Center of Gravity including CG angle with A1 flange plane. See Figure 4-11 and Figure 4-12.

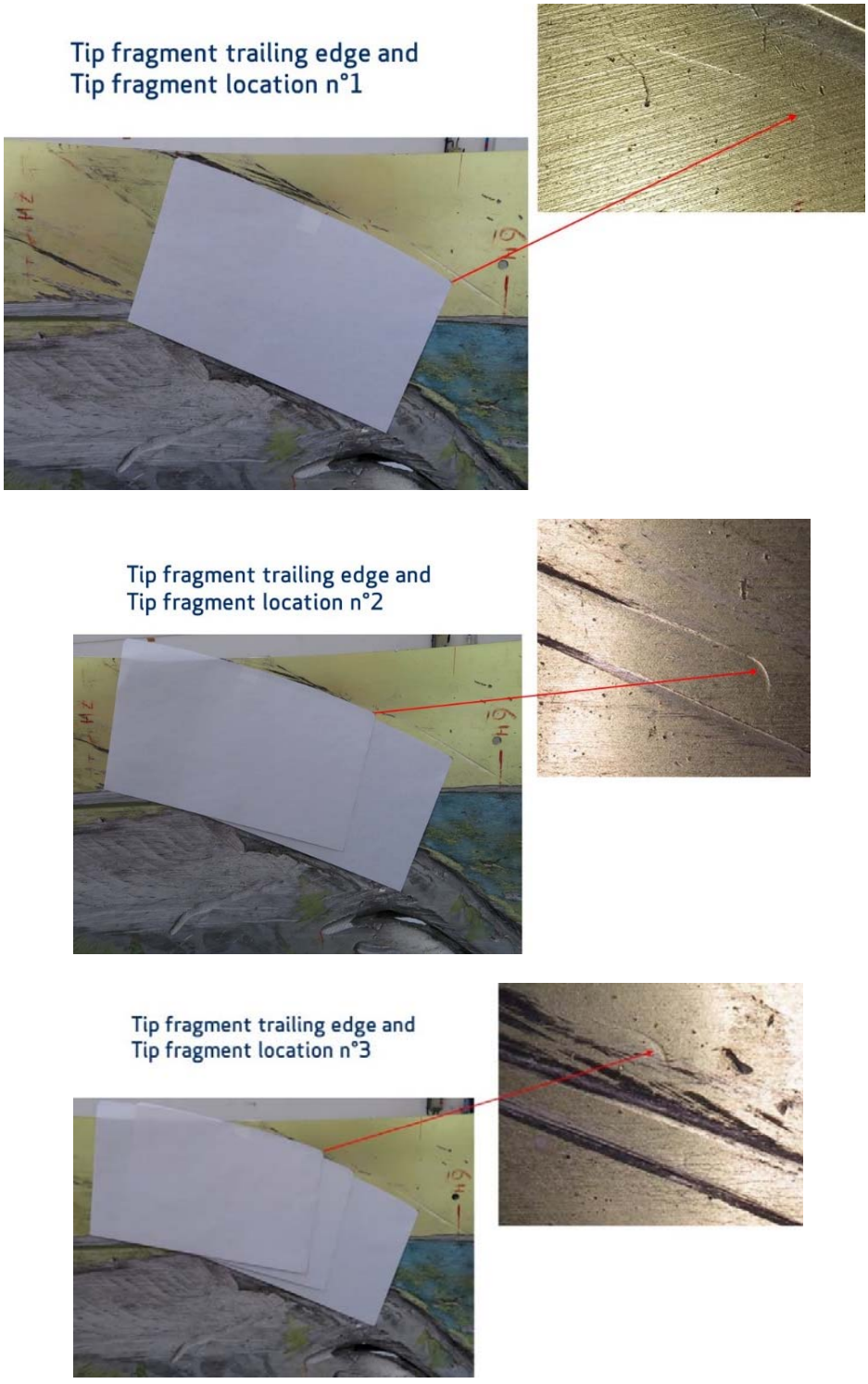

Figure 4-10 : Three distinct locations observed of the tip fragment trailing edge radius on Philadelphia engine 875134 Fan case

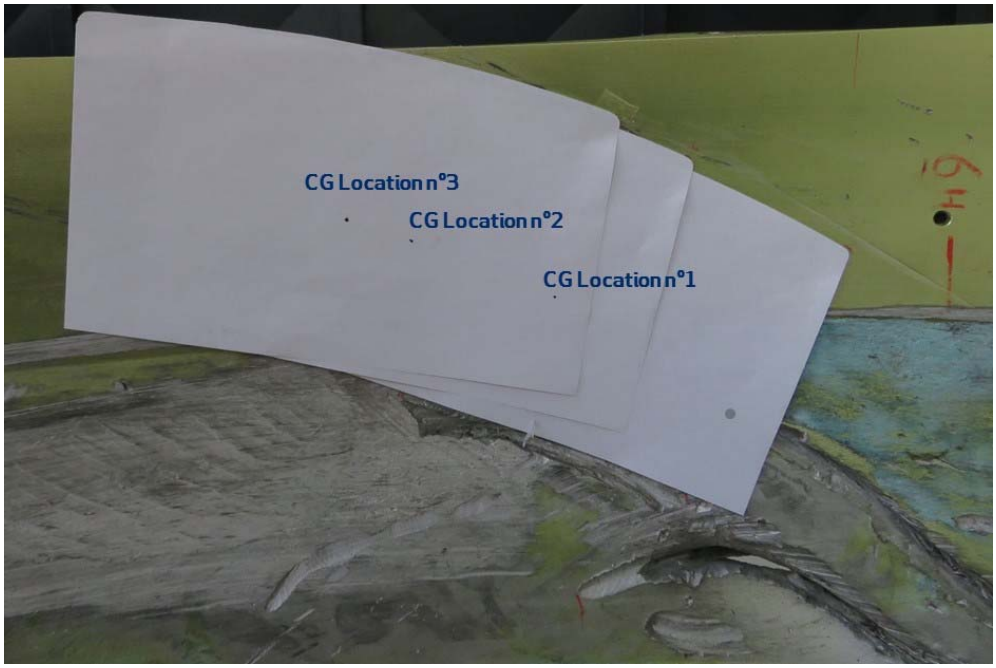

Figure 4-11 : The three distinct locations of the Tip fragment superimposed to show Tip fragment CG trajectory

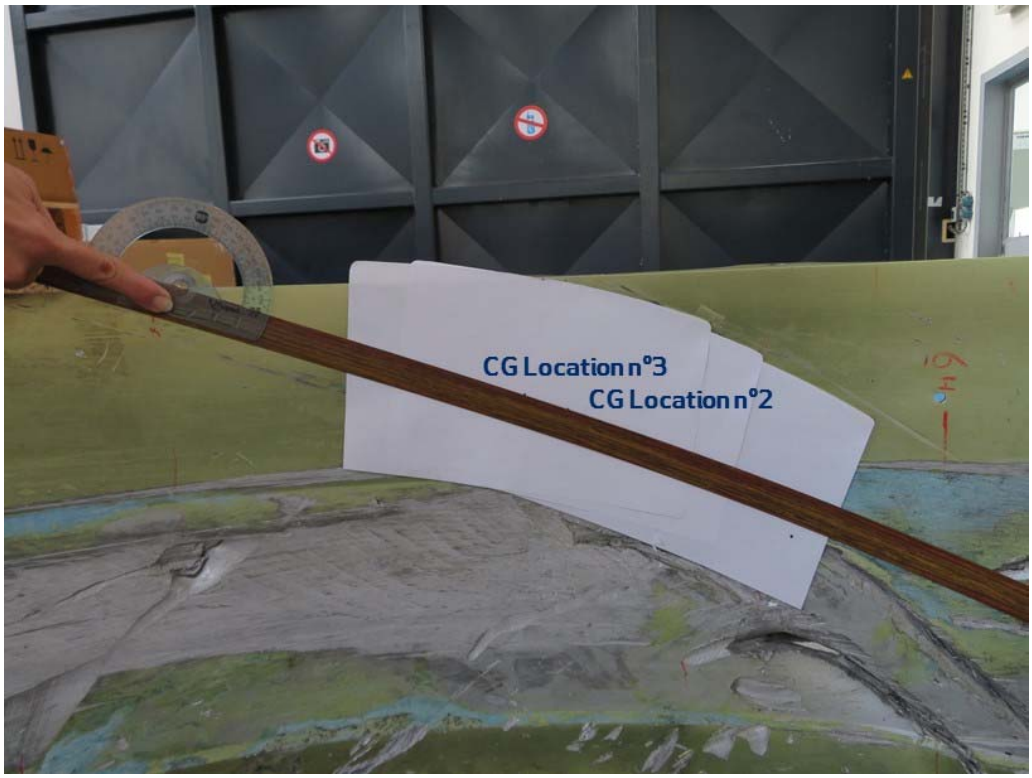

Figure 4-12 : Tip fragment CG trajectory angle measurement

Based on the two most forward identified locations of the Tip fragment *CG* on Philadelphia engine 875134 Fan case (location n°2 and location n°3), the Tip fragment CG trajectory angle crossing A1 Flange is 20°. However, note that from location n°1 to location n°3, the angle of the Tip fragment CG with A1 flange is reducing, so the CG trajectory angle when crossing A1 flange could be lower than 20°.

4.4 Tip fragment trajectory based on LS-DYNA prediction with Philadelphia conditions

The LS-DYNA correlated model has been performed with Philadelphia boundary conditions (N1 speed, blade release angle).

Using Philadelphia conditions, the initial time T = 0ms corresponds to a release angle of 4:30.

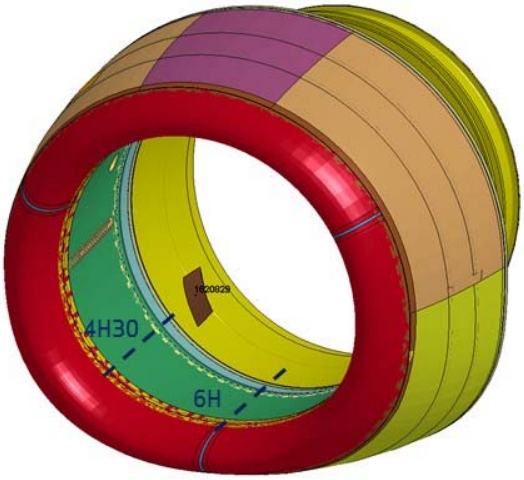

Figure 4-13 : LS-DYNA model in Philadelphia conditions, Tip fragment at T=0ms

LS-DYNA results have been analyzed as follows:

- The Tip fragment CG predicted trajectory is analyzed from the blade release angle up to half a revolution
- The calculated Tip fragment CG trajectory is described on Figure 4-14 and crosses A1 flange at 5ms around 8:10 before half a revolution (5.8ms)

The calculated Tip fragment trajectory between 4:30 and 9:00 is described on Figure 4-14.

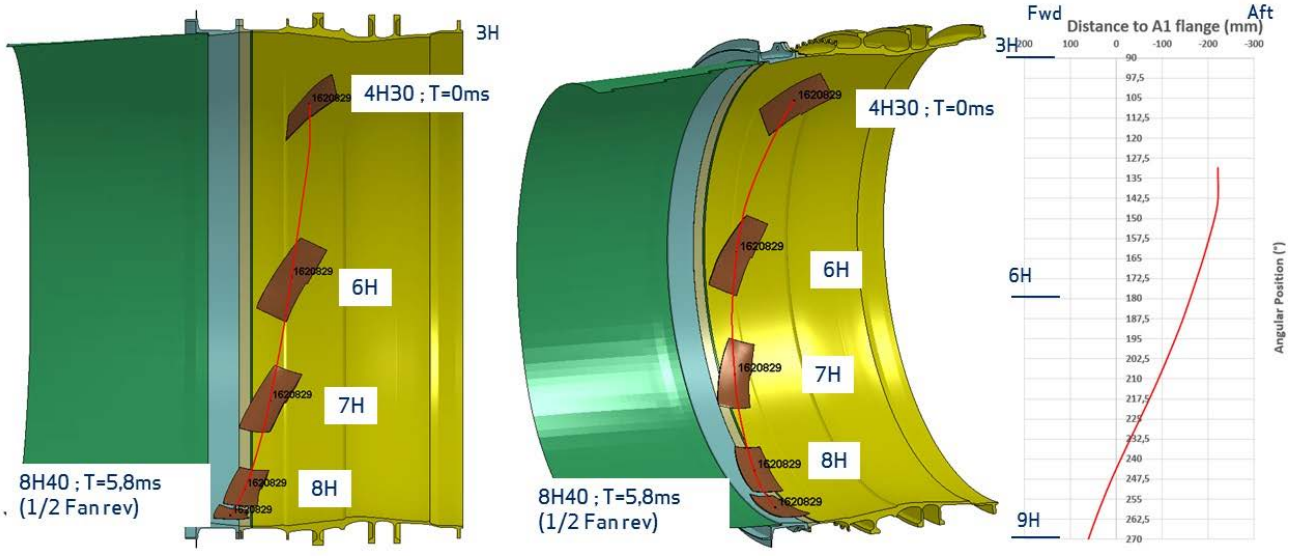

Figure 4-14 : LS-DYNA calculated Tip fragment CG trajectory for Philadelphia engine 875134 conditions

The calculated Tip fragment trajectory and associated angle with A1 flange axial plane is described on Figure 4-15.

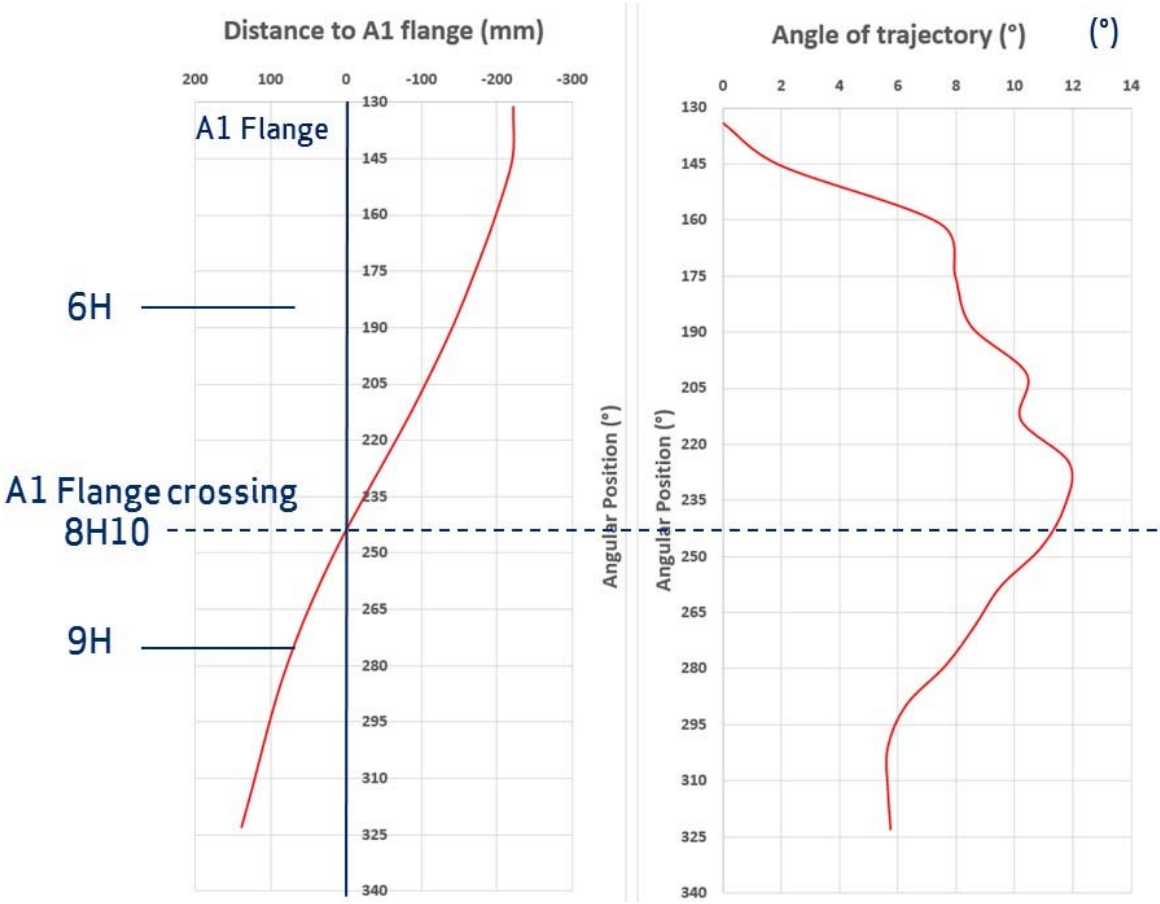

Figure 4-15 : LS-DYNA calculated Tip fragment CG trajectory for Philadelphia conditions

As shown in Figure 4-15, the predicted angles of the CG are as follows:

Tip fragment CG trajectory angle at A1 Flange is 11.1°
The maximum calculated angle before crossing A1 flange is 12°.

The *predicted* Tip fragment CG trajectory angle in Philadelphia conditions (11.1°) is similar to the Tip fragment CG trajectory angle *predicted* on engine 874-002/2 FBO Certification test conditions (13.2°).

As described previously, the Tip fragment CG trajectory *measured* on Philadelphia engine 875134 before crossing A1 flange is 20°. As the Tip fragment CG with A1 flange is reducing when sliding forward to the A1 flange the CG trajectory angle at A1 flange crossing could be lower than 20° (see section 3.1.3).

Conclusion:

LS-DYNA Tip fragment trajectory and associated angle prediction in Philadelphia conditions is similar to the prediction for engine 874-002/2 FBO Certification test conditions.
The LS-DYNA prediction shows a lower but similar (within prediction and measurement error uncertainty) trajectory angle when crossing the A1 flange than Philadelphia engine 875134 visual evidence measurements.

4.5 Tip fragment impact and damage on Inlet A1 flange

Local damage on Inlet A1 flange shows that the tip fragment impacts Inlet A1 flange before entering into the Inlet inner diameter on both the Philadelphia and Pensacola engines, which was not observed during Rig test 4 or certification test 874 002/2.

Figure 4-16 : Inlet A1 flange damaged by tip fragment on Pensacola engine 874112

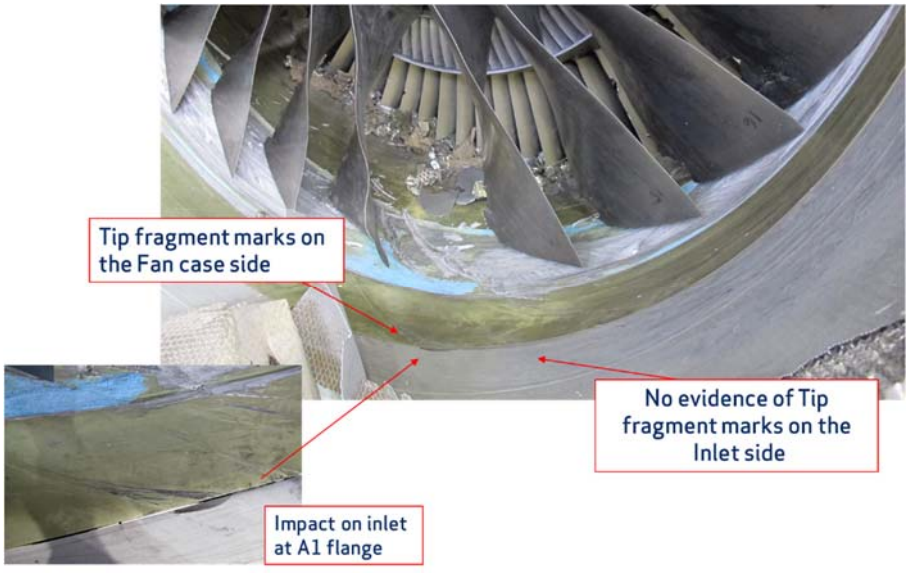

Figure 4-17 : Inlet A1 flange damaged by tip fragment on Philadelphia engine 875134

On Pensacola and on Philadelphia engines, Tip fragment marks observed on the Fan case side are not continuous forward to A1 flange in the Inlet. A damage is noticeable at Inlet A1 flange lip due to Tip fragment impact.
This impact of the Tip fragment on Inlet A1 flange lip would modify the sliding action of the Tip fragment entering the Inlet forward to A1 flange.

Potential effect of Inlet A1 flange Lip impact on Tip fragment trajectory

Physical evidence (witness marks) indicate the Tip impacted the inlet A1 flange lip, and sheared the "corner" of the flange resulting in a "divot" of missing material. A potential result of the impact is that the tip panel goes airborne (in lieu of continuing to slide) as shown in Figure 4-18.

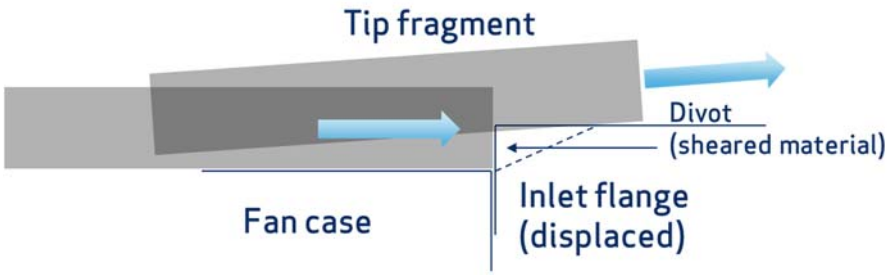

Figure 4-18 : Tip fragment entering inlet – Trajectory changed due to inlet flange displacement and damage to the inlet flange lip

Figure 4-19 describes the tip fragment theoretical axial location based on trajectory of a ball rolling in a cone. If the fragment loses contact with inlet when crossing A1 flange, it results in more forward trajectory of tip fragment.

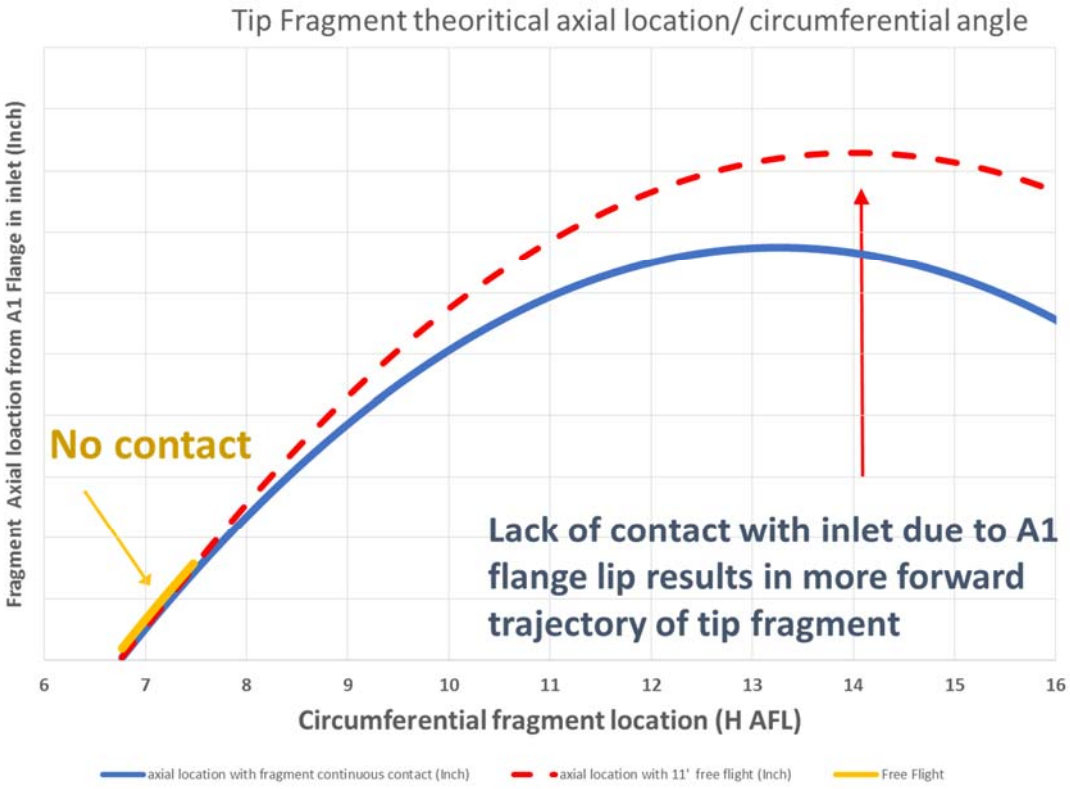

Figure 4-19 : Tip fragment theoretical axial location in inlet versus circumferential angle

Loss of contact with inlet A1 Flange lip also results in no friction between fragment and inlet. This results in higher velocity and increased energy of the fragment further forward in the inlet compared to certification test.

Therefore, the tip fragment impact with A1 flange aft facing step likely resulted in more forward fragment trajectory in the inlet.

4.6 Conclusions

For Pensacola and Philadelphia events, the angle of last tip fragment edge witness mark on the fan case in the A1 flange area measure 14 and 15° respectively

However, for Pensacola due to the limited length of the Tip fragment marks it is difficult to determine if trajectory and angle at A1 flange of tip fragment *edge* is completely representative of the Tip fragment *CG* trajectory.

For Philadelphia, three tip fragment edge imprints have been observed on fan case that help build a tip fragment trajectory when crossing A1 flange. Based on the two last locations of tip fragment observed, the Tip fragment CG trajectory angle crossing A1 Flange is 20°. However, note that from the first location to the third location of tip fragment observed, the angle of the Tip fragment CG with A1 flange is reducing, so the CG trajectory angle when crossing A1 flange could be lower than 20°.

Damage at A1 inlet flange lip has been observed at tip fragment crossing from fan case to inlet. This tip fragment impact with A1 flange aft facing step could have resulted in more forward fragment trajectory in the inlet and increased fragment energy forward in inlet.

Section 5.0 Mid Fragments trajectories

5.1 Mid fragments trajectory on Pensacola engine 874112

Details about mid span fragments trajectory for Pensacola are included in Airworthiness Group Chairman's Factual Report–Attachment 3 – NTSB DCA16FA217.
Based on witness marks, two mid span fragments trajectories have been identified on Pensacola engine 874112 fan case.
One trajectory path exits at 8 o'clock with an exit angle of 6° versus A1 flange as shown in Figure 5-1.
Note:

- Local, permanent, deformation of the fan case along the mid panel trajectory is observed
- Deformation causes deviation of the trajectory
- Direct measurement of the exiting angle at the A1 flange location : 6°
- Exiting angle with linear trajectory based on the marks between abradable and A1 flange : 8°

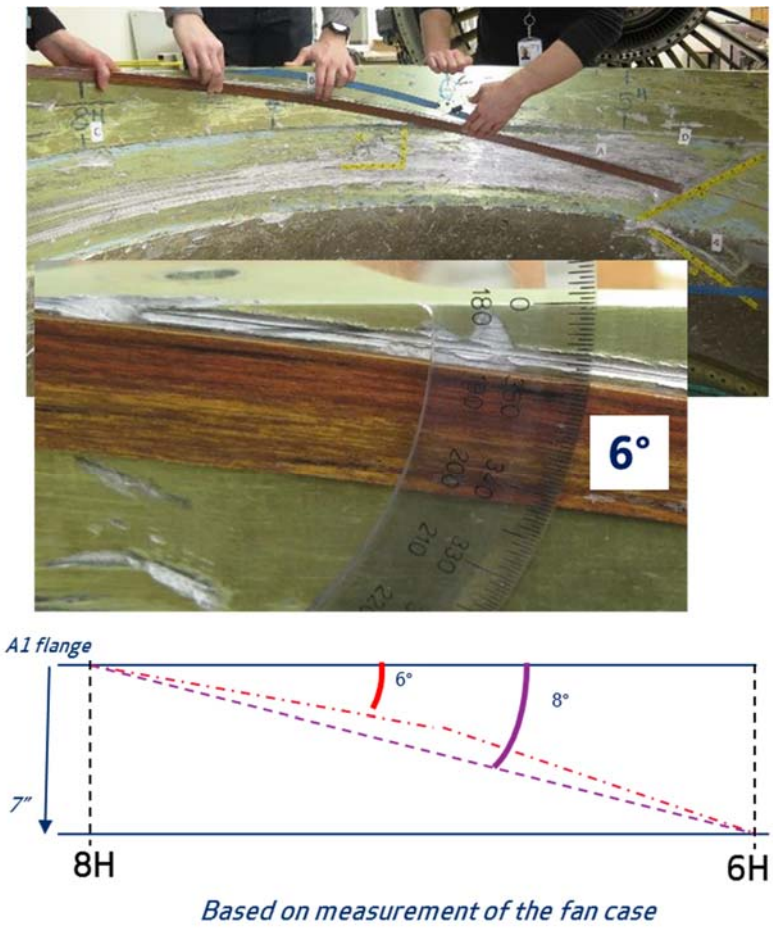

Figure 5-1 : Pensacola engine 874112 Fan case Mid fragment mark exiting at 8:00 / Measured angle at A1 flange

Multiple marks in the area of 4:30 suggest also some mid span fragments were ejected in this area.
The measured angle of one Mid fragment trajectory with A1 flange plane is 37° as shown on Figure 5-2.

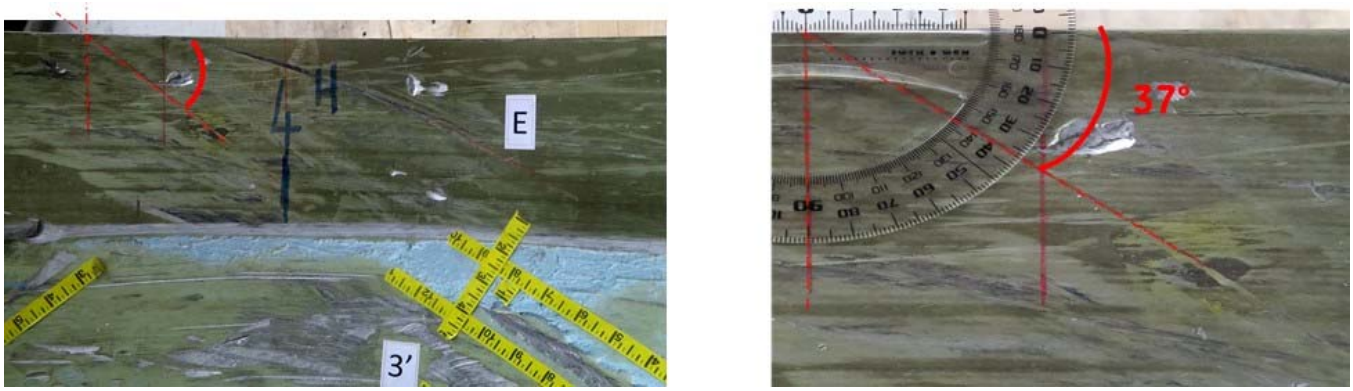

Figure 5-2 : Pensacola engine 874112 Fan case Mid fragments marks and measured angle at A1 flange

5.2 Mid fragments trajectory on Philadelphia engine 875134

Philadelphia engine 875134 shows mid fragments marks on the Fan case and on the Inlet.

The angle of these Mid fragments witness marks on the Fan case side have been measured and are the described in Figure 5-3 and 5-4.

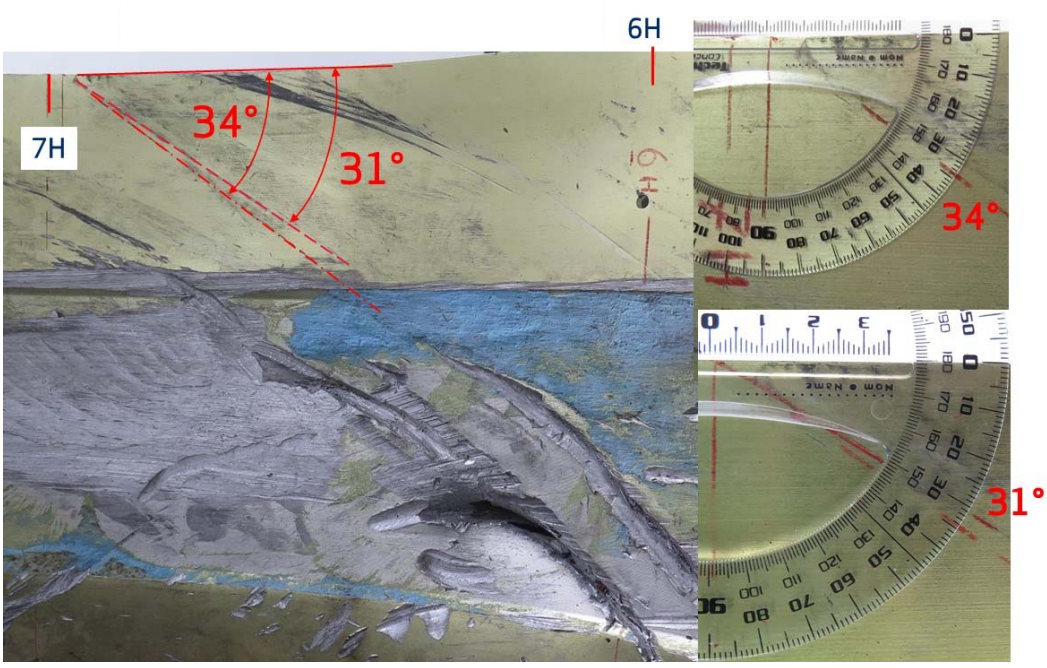

Figure 5-3 : Philadelphia engine 875134 Fan case Mid fragments marks and measured angle at A1 flange at 7:00

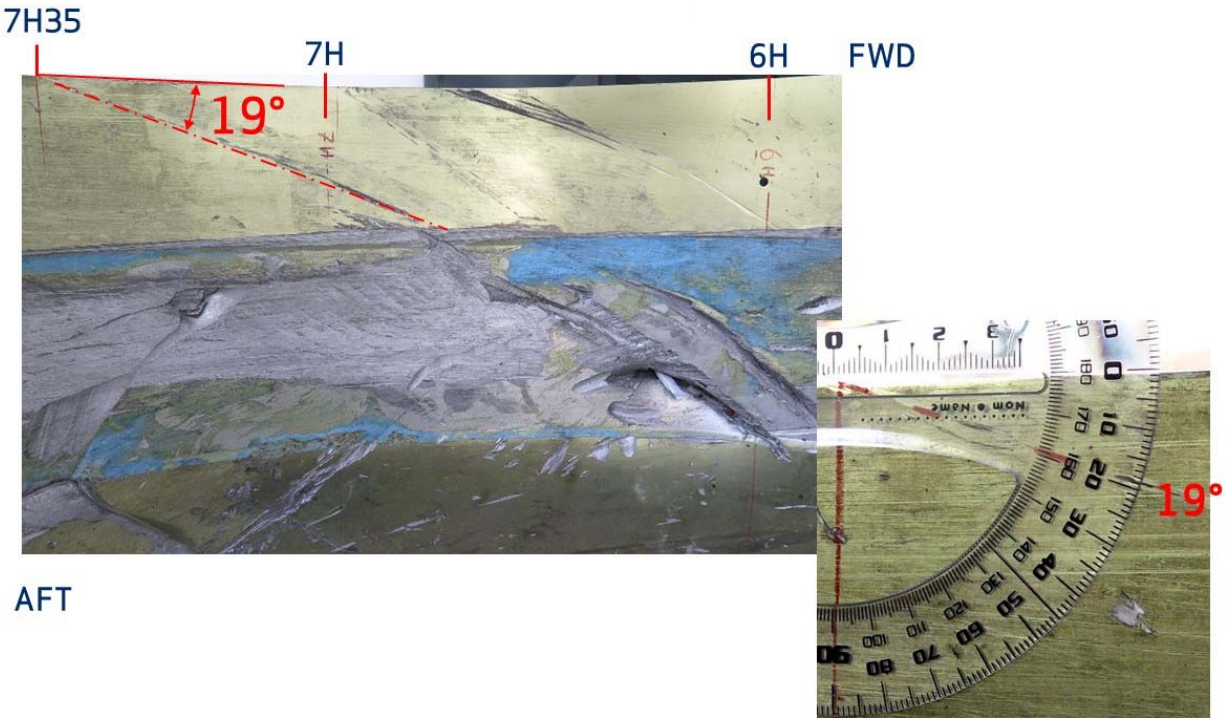

Figure 5-4 : Philadelphia engine 875134 Fan case mid fragments marks and measured angle at A1 flange at 7:35

Visual evidence of two/three mid fragment trajectories going forward have been observed on both Pensacola and Philadelphia engines fan cases. The exit angles when crossing A1 flange vary from 6° to 37° including data from both events.

6.1 Inlet Damage Assessment Introduction

The NTSB Structures parties have met multiple times at the UTAS facility in Chula Vista with the objective to determine the areas in the Philadelphia event inlet (Figure 3.1.1) primarily on the inner barrel, which were damaged due to fan blade fragments versus areas, which were damaged due to subsequent damage propagation and the inlet separation. The damage areas considered were the inner barrel perforated skin and honey comb, and the inner barrel backskin just forward of the inner barrel containment doubler. Primary participants were Boeing, CFM and UTAS. The UTAS metallurgical laboratory supported the objective with detailed metallurgical studies of areas of the separation plane
The following pages summarize the CFM perspective on this activity.

Figure 6-1 : Inlet condition Post event

Figure 6-2 : Philadelphia Inlet in UTAS Facility

Section 7.0 Inlet Inner Barrel Damage Assessment

In order to enable the Boeing progressive damage analysis to proceed in parallel with the separation plane damage assessment, the parties defined an *initial* range of damage assessments.

Three levels of potential damage were defined during the Oct. NTSB meeting at UTAS based primarily on the UTAS metallurgical analysis of inlet damaged areas which had been completed at that time.

These levels were defined as Phase 1, 2, and 3, in decreasing order of certainty based on macro visual inspection and UTAS laboratory results.

Phase 1 – "Damage Supported by Hard Evidence": Per the Boeing/UTAS definition, the evidence includes the presence of Titanium found on the Outer Barrel supporting damage up to 11:00; it was then extended out to 12:45 where the "radially out" fracture surface changes to "alternating".

Phase 2 – "Damage Supported by Fracture Surface Evidence & Titanium Findings, possibly from fragments"

Phase 3 – "Damage Supported by Hypothesis of Fragment Damage Progression"

These damage levels are summarized in Figure 7-1. Fracture zones where the material was bent radially outward were considered indicative of fragment penetration. These initial damage assessments did not include the trajectories of the fan blade fragments and the evidence of fragments being present in the area of damage (or not).

The following pages integrates CFM fragment trajectory understanding and additional hardware observations to the UTAS metallurgical findings to refine potential fragment damage area definition. To support the analysis, several Figures are included which are directly extracted from UTAS material presented in team meetings.

Input Damage to LS Model Analysis Sensitivity Studies						
			Perf Skin	Back Skin Damage		
Sample Area	Clock (ALF)	Back Skin Directionality	Phase (1 - 3)	Phase 1	Phase 2	Phase 3
1	5:00	Alt				
2	6:00	Alt				
3	6:45	Tensile				
4	7:00	Alt				
*	7:30	Radial Out				
5	8:00	Radial Out				
6	8:30	Radial Out				
*	8:45	Alt				
7	9:00	Alt				
8	9:30	Alt				
10	10:00	Alt				
11	10:30	Radial Out				
12	11:00	Radial Out				
13	11:30	CW Rad Inbd.				
14	12:00	Radial Out				
16	12:30	Radial Out				
*	12:45	Radial Out				
17	1:00	Alt				
* Average between adjacent clock locations (Transition Point)						

Figure 7-1 : Three Phases Characterization of Separation Plane

(Reference Oct. 2018 Structures Team Meeting)

Section 8.0 Phase 1 Inlet Damage Assessment

8.1 Phase 1 inlet Damage Assessment – Introduction

The Boeing/UTAS definition of the Phase 1 inner barrel back skin damage area at the conclusion of the October 2019 meeting at UTAS was:
Phase 1 -Damage Supported by Hard Evidence
Titanium found on the Outer Barrel provides hard evidence of inner barrel back side skin damage up to 11:00, which is then extended out to 12:45 where the “radially out” fracture surface changes to “alternating”.
The fore aft width of 1.0 inch is an average of the areas with fragment penetration (assumed 2.0 inch) and areas that have “unzipped” (assumed dimensionless).

UTAS documented the inner barrel fracture surface at specific clock locations around the Phase 1 area. These locations are shown in Figure 8-1.

CFM has combined the data from the UTAS metallurgical results with the latest CFM fragment trajectory evaluation, along with additional hardware observations gathered during Structures party examinations of the inlet hardware at UTAS to make an updated assessment of the Phase 1 damage.

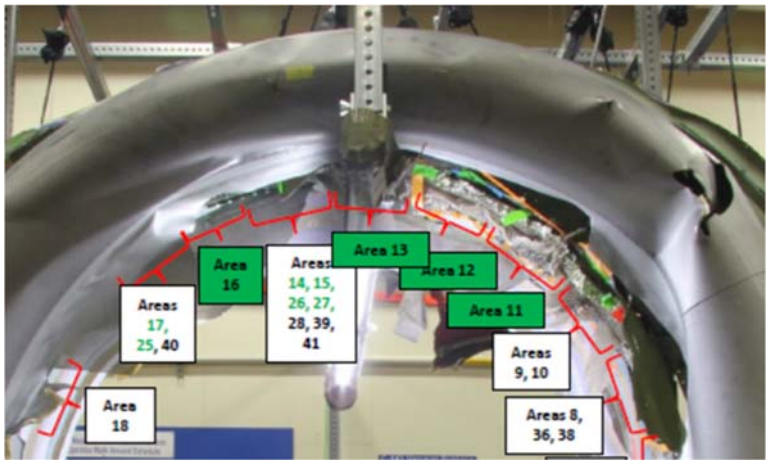

Figure 8-1 : Phase 1 Metallugical Areas

(Reference Oct. 2018 Structures Team Meeting)

8.2 Phase I Inner Barrel Fracture Surface: Assessment of inner barrel fracture surface around Phase1 damage zone from UTAS metallurgical results and visual observations at specific clock positions

9:30 Position, Area 8. Outside of Boeing Phase 1 area. See Figure 8-2.
UTAS metallurgical results showed alternating directions of backskin fracture surface shear. Visual inspection showed that the backskin fracture was inside and aft of the intact containment doubler forward edge. This indicates that the backskin fracture could not be due to fragment penetration.

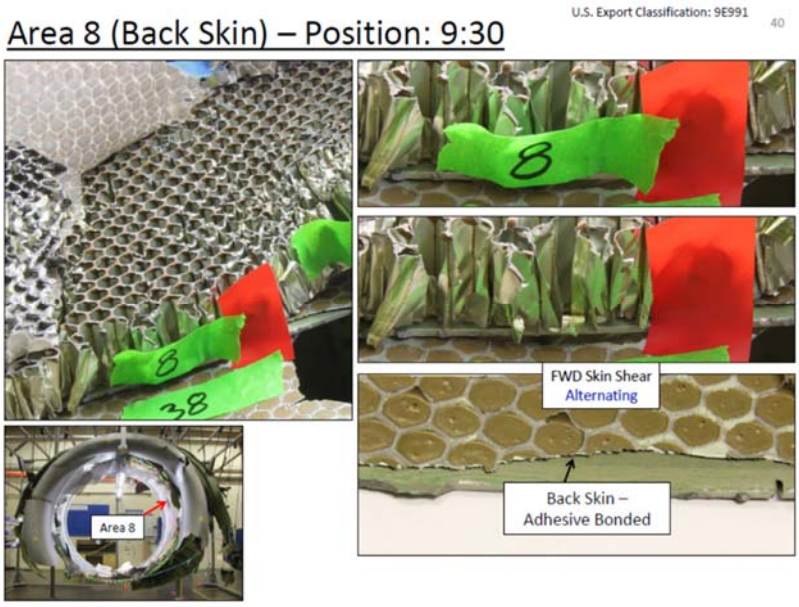

Figure 8-2 : Position 9:30

(Reference Oct. 2018 Structures Team Meeting)

10:30 Position, Area 11. Start of Boeing Phase 1 area. See Figure 8-3

UTAS metallurgical results showed radial outboard direction of backskin fracture surface shear. Visual inspection shows backskin fracture at forward edge of containment doubler, with backskin deformed radially outward. There is technical basis to conclude that this damage is due to fragment penetration.

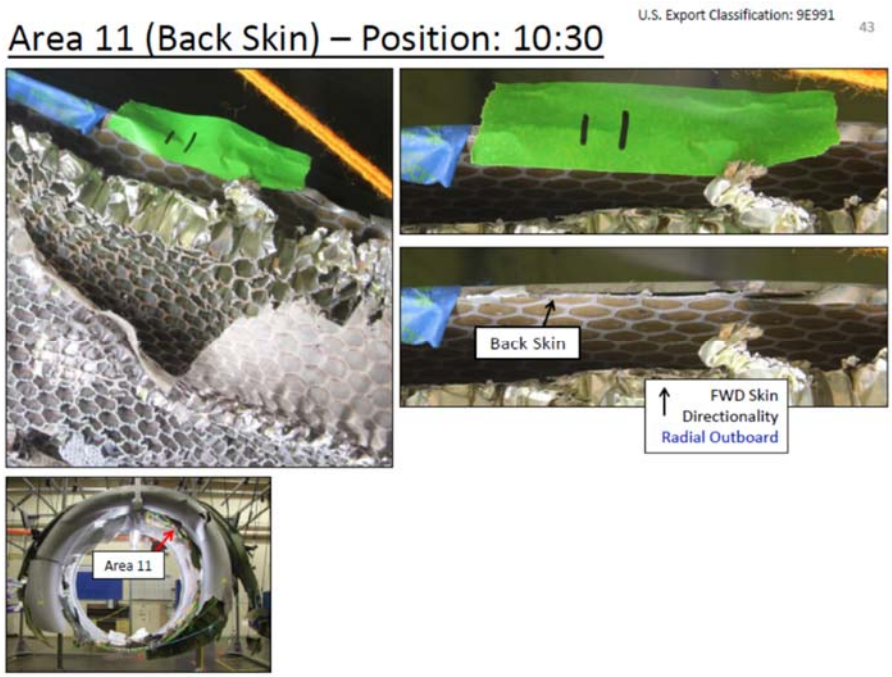

Figure 8-3 : Position 10:30

(Reference Oct. 2018 Structures Team Meeting)

11:00 Position, Area 12. Within Boeing Phase 1 area. See Figure 8-4

UTAS metallurgical results showed radial outboard direction of backskin fracture surface shear. Visual inspection shows backskin fracture at forward edge of containment doubler, with backskin and edge of doubler deformed radially outward. Titanium alloy particles were found on the deformed edge. There is technical basis to conclude that this damage is due to fragment penetration.

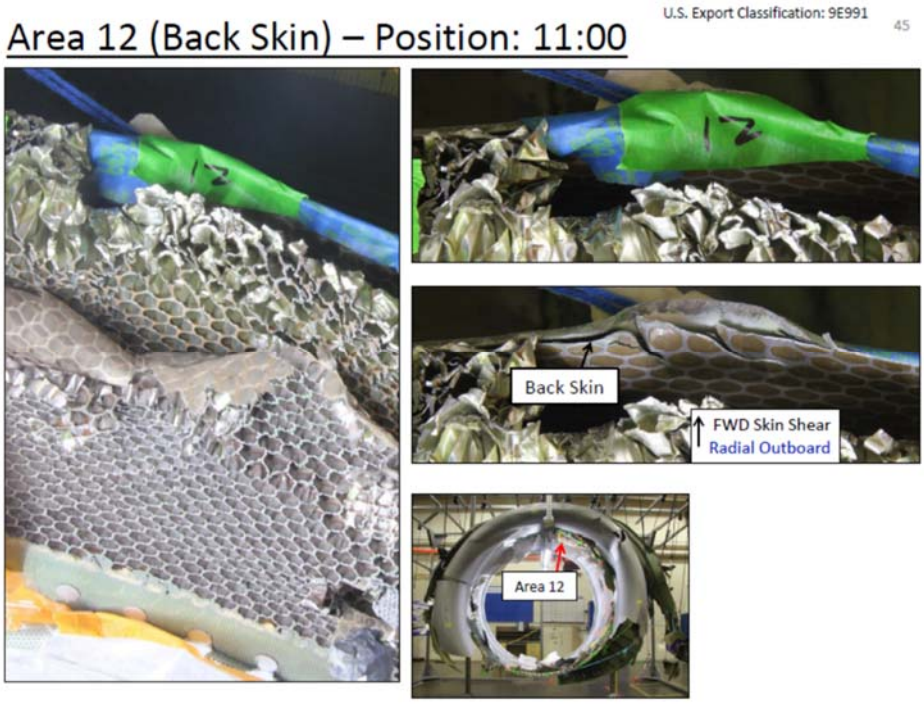

Figure 8-4 : Position 11:00

(Reference Oct. 2018 Structures Team Meeting)

11:30 Position, Area 13. Within Boeing Phase 1 area. See Figure 8-5

UTAS metallurgical results showed tangential radial inward direction of backskin fracture surface shear. This is not consistent with fragment penetration.

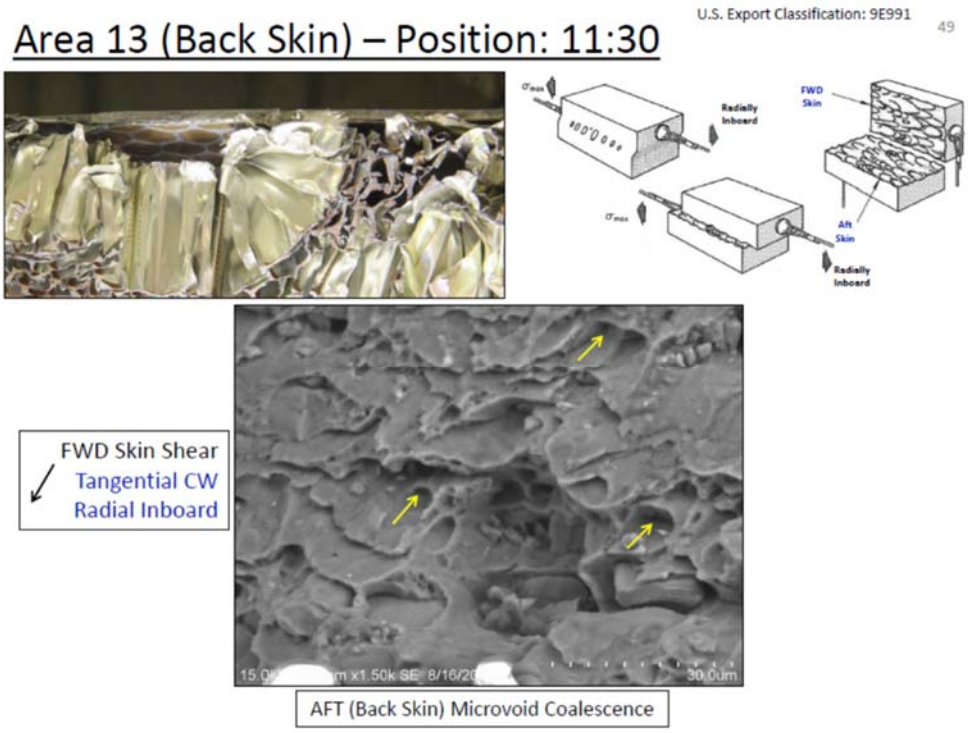

Figure 8-5 : Position 11:30

(Reference Oct. 2018 Structures Team Meeting)

12:00 Position, Area 15. Within Boeing Phase 1 area. See Figure 8-6

UTAS metallurgical results showed radial outboard direction of backskin fracture surface shear. Macro visual inspection shows that the backskin is not deformed in radial outward direction. The honeycomb core is not deformed radially. These conditions are not consistent with fragment penetration.

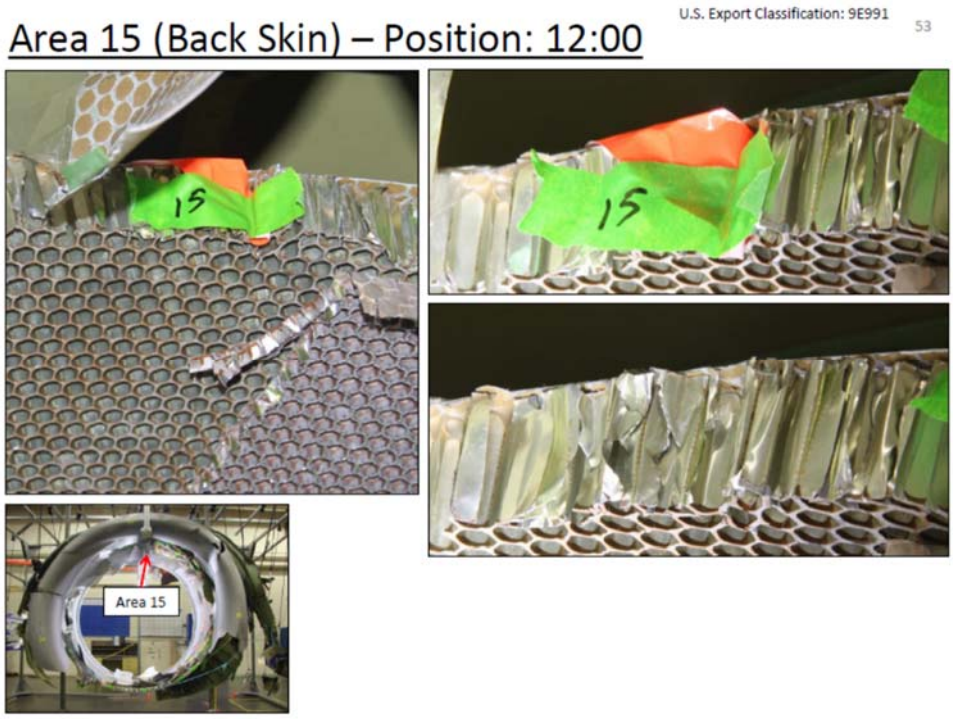

Figure 8-6 : Position 12:00

(Reference Oct. 2018 Structures Team Meeting)

12:30 Position, Area 16. Within Boeing Phase 1 area. See Figure 3.2.8

UTAS metallurgical results showed radial outboard direction of backskin fracture surface shear. Macro visual inspection shows that the backskin is not deformed in radial outward direction. The honeycomb core is not deformed radially. These conditions are not consistent with fragment penetration.

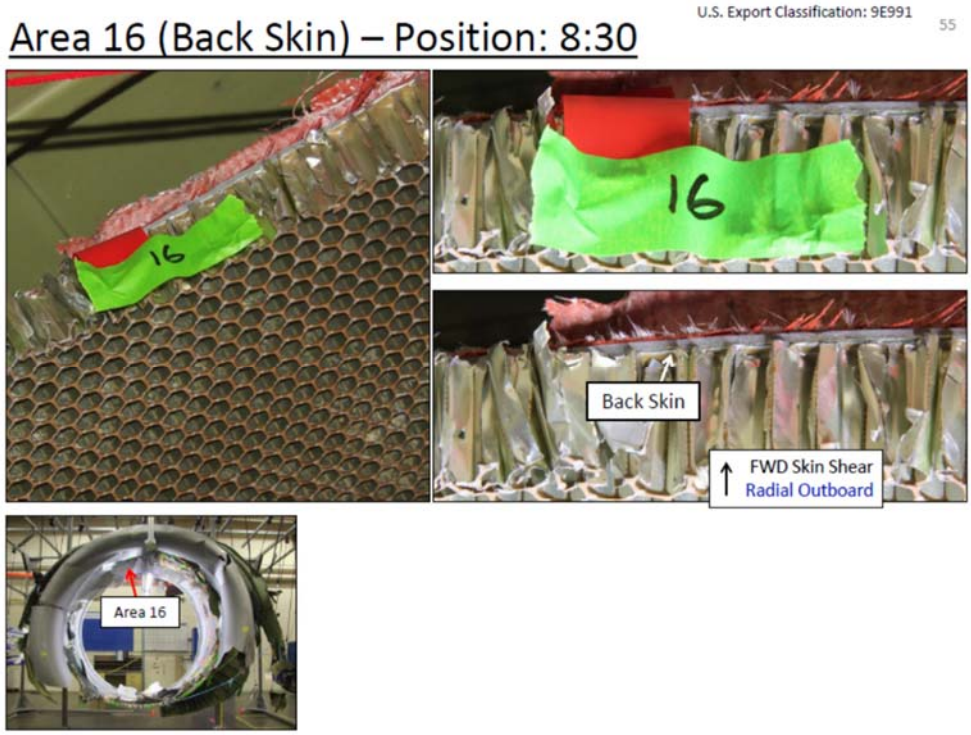

Figure 8-7 : Position 12:30

(Reference Oct. 2018 Structures Team Meeting)

8.3 Phase 1 Outer Barrel Penetration

The inlet outer barrel exhibited damage at 12:00 and 12:30. Both locations contained titanium particles. These locations are consistent with fragment trajectories leaving the inner barrel between 10:30 and 11:00. See Figure 8-8. This outer barrel damage supports inner barrel fragment penetration between 10:30 and 11:00.

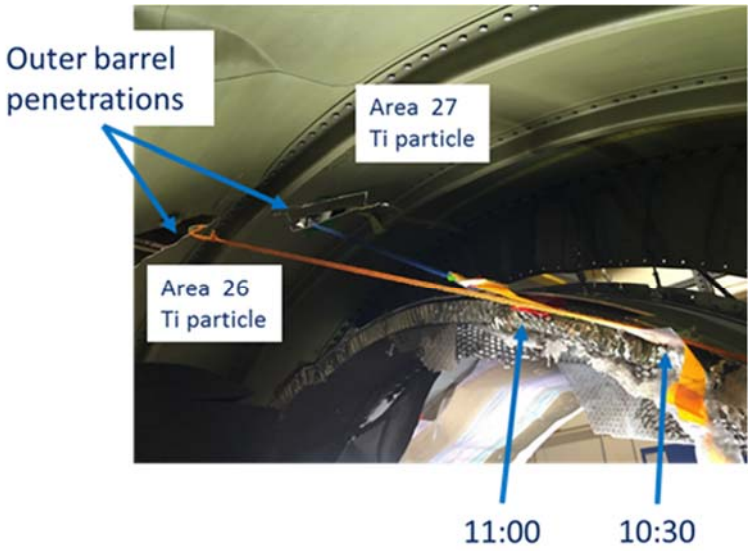

Figure 8-8 : Position 11:30 Outer barrel

(Reference Oct. 2018 Structures Team Meeting)

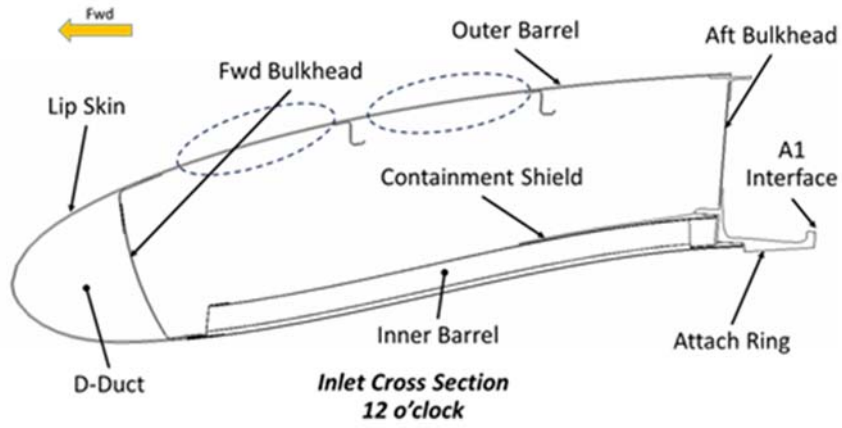

Figure 8-9 Inlet cross section at 12 o'clock

(Reference Oct. 2018 Structures Team Meeting)

8.4 Propagation Behavior Adjacent to Penetration

Phase 1 Boeing definition was stated as based on "hard evidence of inner barrel back side skin damage up to 11:00, which is then extended out to 12:45". The extended area assumed instantaneous "unzipping" or propagation of the backskin adjacent to penetration damage.
No specific data was stated to support the assumption of instantaneous propagation of the penetration damage.
The expected propagation behavior of the inner barrel adjacent to a fragment penetration can be inferred from the outer barrel penetration at 12:00. This is believed to be caused by one of the fragments that penetrated the inner barrel near 11:00 and subsequently penetrated the outer barrel. Both the inner barrel and outer barrel are made from the same AL 2024 material. The outer barrel did not exhibit apparent unzipping or propagation adjacent to the ballistic penetration

damage. Therefore, it should not be assumed without any supporting technical data that the inner barrel damage unzipped or propagated beyond the fragment penetration.

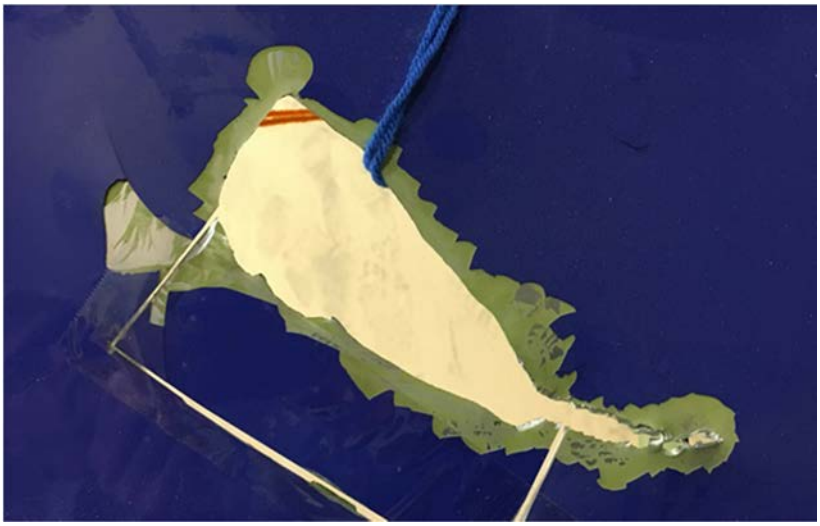

Figure 8-10 Outer barrel fragment penetration at 12:00

(Reference Oct. 2018 Structures Team Meeting)

8.5 Fragment trajectories within inlet

Fan blade fragment trajectories entering the inlet were determined by CFM from sliding and contact marks in the fan case, combined with LS-DYNA analysis and certification test data. The fragment trajectories were communicated in the CFM fragment White Paper of October, 2018, and are documented in sections 4 and 5 of this report. The evidence shows that three/four fan blade fragments traveled forward into the inlet, one tip panel fragment and two/three midspan fragments.

The orientation and trajectory of the tip panel was clearly determined from distinct contact marks on the fan case caused by the blade TE to tip corner radius (see Figure 4-10). The tip fragment center of gravity trajectory angle was determined from these witness marks to be maximum 20 degrees as it entered the inlet. The witness marks also showed that the tip fragment was sliding in a flatwise position, with the tip edge forward and the trailing edge to the left (forward looking aft). Therefore, the trajectory angle and orientation of the tip fragment *is known* as it enters the inlet as shown in Figure 8-11. The tip panel helix angle is assumed to reduce once inside the inlet due to the effect of the inlet cone angle on the trajectory (See figure 4-15 or figure 4-19). The resultant trajectory of the tip fragment in the inlet is consistent with damage marks on the inlet attach ring and perf skin indicating sliding contact with a fragment with significant size and radial load.

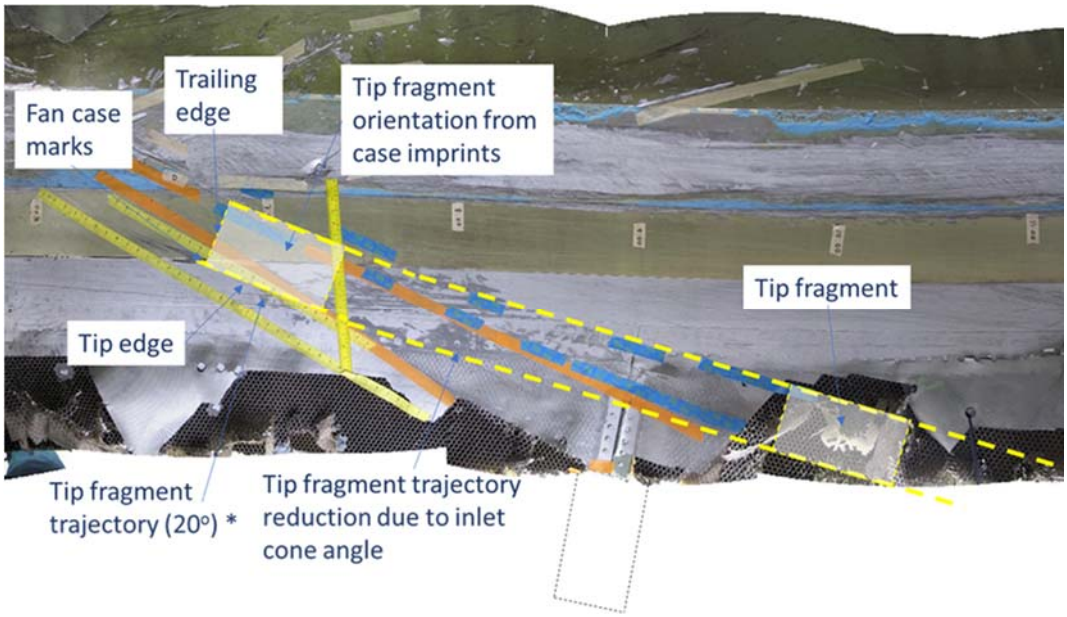

Figure 8-11 Tip panel direction and orientation

The trajectories of the mid span fragments were also determined from distinct sliding contact marks on the fan case (see paragraph 5-2). Two mid span fragments were determined to have gone forward into the inlet and potentially a third one also (see section 2). The fragment trajectory angles were determined to be 31-34 degrees, and 19 degrees.

The 31-34degree mid span trajectories align with the edge of contact damage to the perf skin and honeycomb, as shown in figure 8-12. To the left of the fragment edge trajectory, there is no evidence of honeycomb crushing, or perf skin damage. To the right of the trajectory line there is clear perf skin damage from sliding contact and honeycomb radial crushing indicating outward radial load consistent with a sliding fragment. The mid span fragment at 31-34 degree trajectory crossed the edge of the containment doubler at the location of the 9:00 inner barrel splice plate, which was intact (although bent back by subsequent D duct contact later in event). These fragments therefore could not have penetrated the inner barrel back skin.

The19 degree mid span fragment aligns with the right most edge of contact damage to the perf skin. It crosses the forward edge of the containment doubler at approximately 10:30.

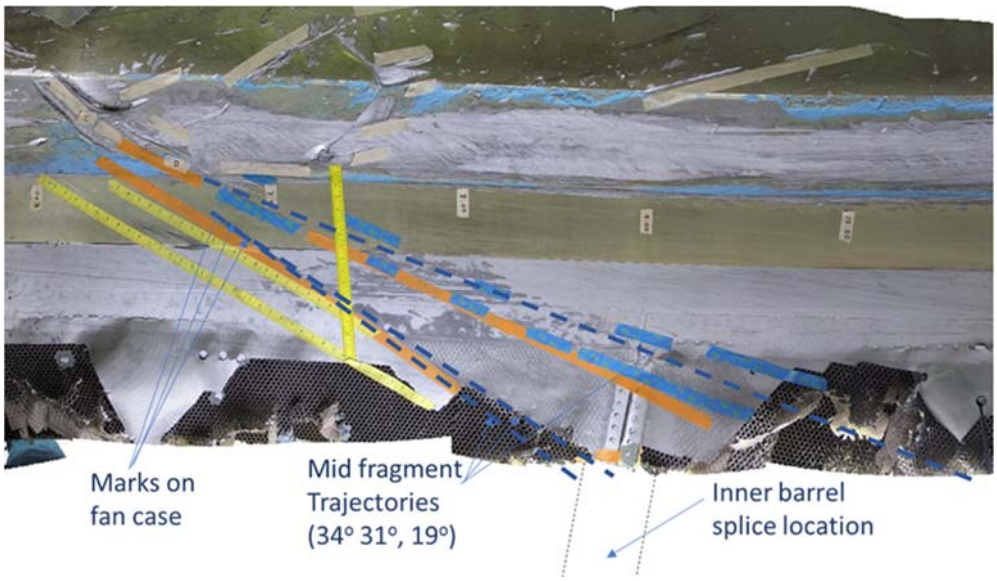

Figure 8-12 Mid span fragment trajectories

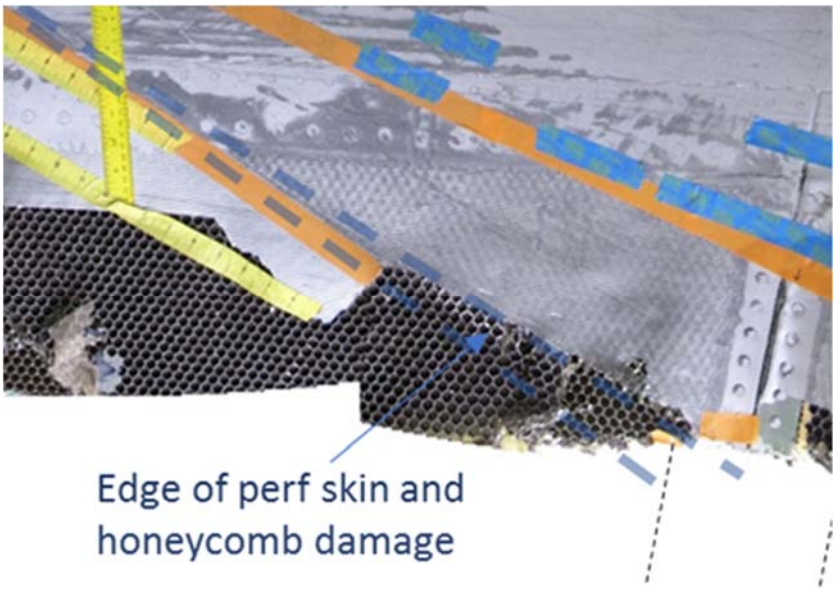

Figure 8-13 Perf skin damage boundaries

8.6 Phase 1 Damage Assessment: Conclusions

The evidence from the metallurgical analysis, macro visual condition, fragment trajectory paths, and hardware observations relating to the Phase 1 damage zone extent are combined on Figure 8-14. The evidence supports that there was Phase 1 fragment penetration of the back skin from approximately 10:30 to 11:30, for a total of 30 degrees. This damage was most likely caused by the tip fragment, with one mid span fragment subsequently passing through the penetration area. This behavior is very similar to the certification and development experience, with the exception of the increased forward travel of the tip fragment. The damage from 11:30 to 12:45 is not consistent with the fragment trajectories or fragment damage. The damage from 11:30 to 12:45 is therefore most likely not due to fragment penetration.

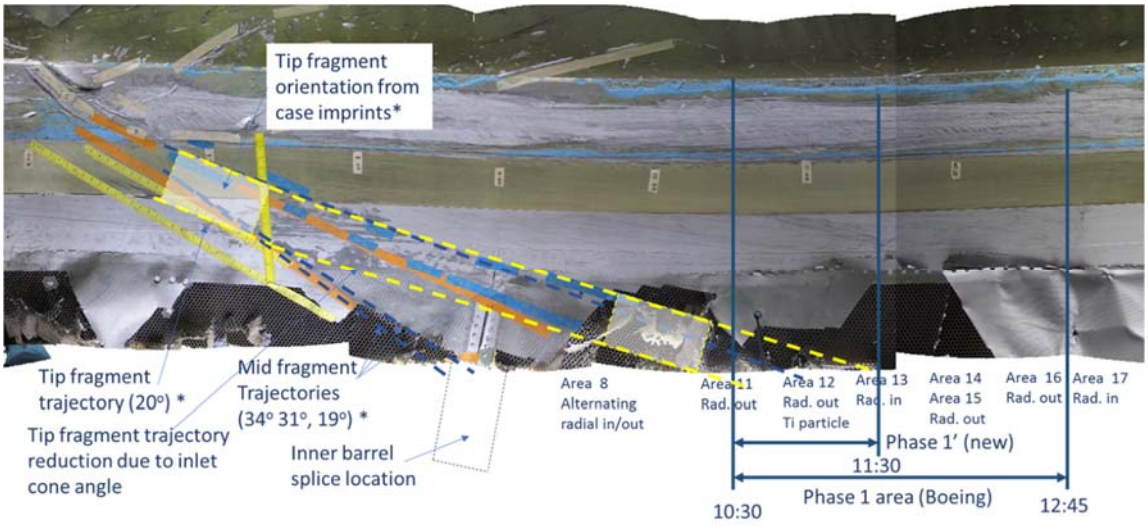

Figure 8-14 Phase 1 damage observations

Section 9.0 Phase 2 Inlet Damage Assessment

9.1 Phase 2 Damage Assessment - Introduction

The Boeing/UTAS definition of the Phase 2 inner barrel backskin damage area at the conclusion of the October 2018 meeting at UTAS was:

> Phase 2 -Damage Supported by Fracture Surface Evidence & Titanium Findings, possibly from fragments
> Backside skin
> Add a circumferential cut in the backside skin, located just forward of the containment doubler forward edge, from 7.30 to 8:30 (9o/c splice) with a 1.0 inch fore-aft width.
> Damage based on possible titanium on outer barrel at 8:30 and radially out fracture surfaces that are similar to 10:30 to 12:45 fracture surfaces.

UTAS documented the inner barrel fracture surface at specific clock locations around the Phase 2 area. These locations are shown in Figure 9-1.

CFM has combined the data from the UTAS metallurgical results with the latest CFM fragment trajectory evaluation, along with additional hardware observations gathered during Structures party examinations of the inlet hardware at UTAS.

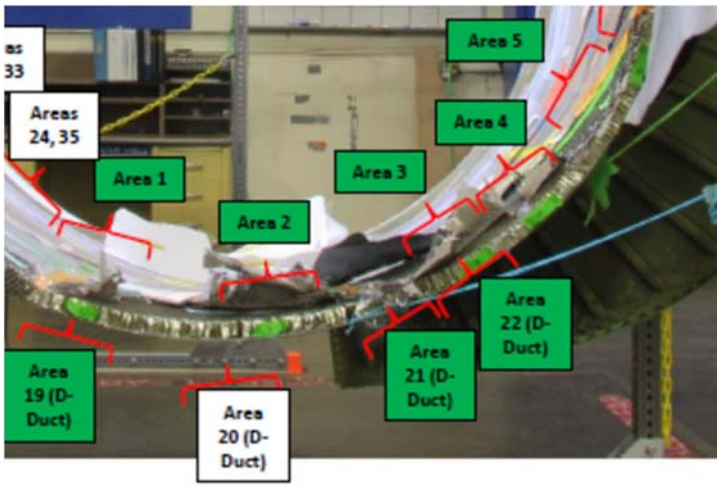

Figure 9-1 Phase 2 Metallurgical areas

(Reference Oct 2018 Structures Team meeting)

9.2 Phase 2 Inner Barrel Fracture Surface: Assessment of inner barrel fracture surface around Phase2 damage zone from UTAS metallurgical results and visual observations at specific clock positions

7:30 Position, Area 4/Area 22. Beginning of Phase 2 area. See Figure 9-2

UTAS metallurgical results showed radially inward direction of backskin fracture surface shear. Macro visual inspection shows that the backskin is not deformed in radial outward direction. The honeycomb core is not deformed radially. These conditions are not consistent with fragment penetration.

Figure 9-2 Position 7:30

(Reference Oct 2018 Structures Team meeting)

8:00 Position, Area 5. Center of Phase 2 area. See Figure 9-3

UTAS metallurgical results showed radially outward direction of backskin fracture surface shear. Macro visual inspection shows that the backskin is not deformed in radial outward direction. The honeycomb core is not deformed radially. These conditions are not consistent with fragment penetration.

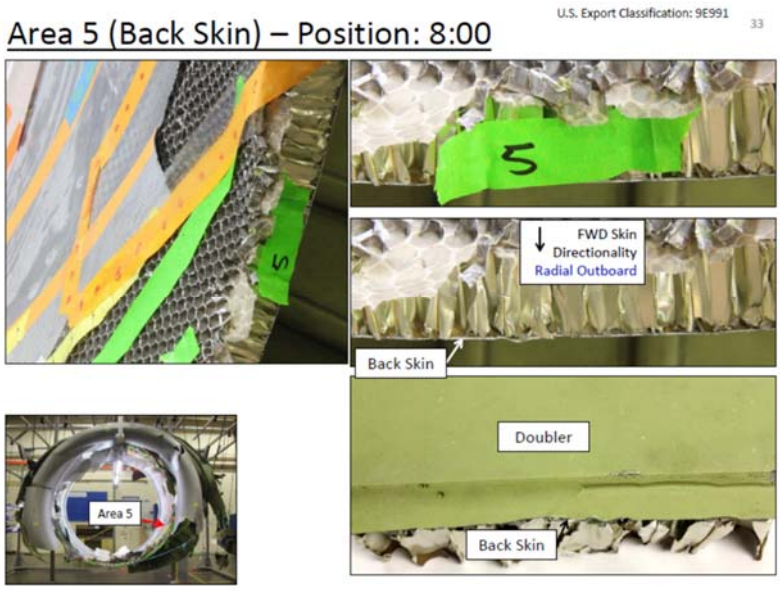

Figure 9-3 Position 08:00

(Reference Oct 2018 Structures Team meeting)

8:30 Position, Area 5. End of Phase 2 area. See Figure 9-4

UTAS metallurgical results showed radially outward direction of backskin fracture surface shear. Macro visual inspection shows that the backskin is not deformed in radial outward direction. The honeycomb core is not deformed radially. These conditions are not consistent with fragment penetration.

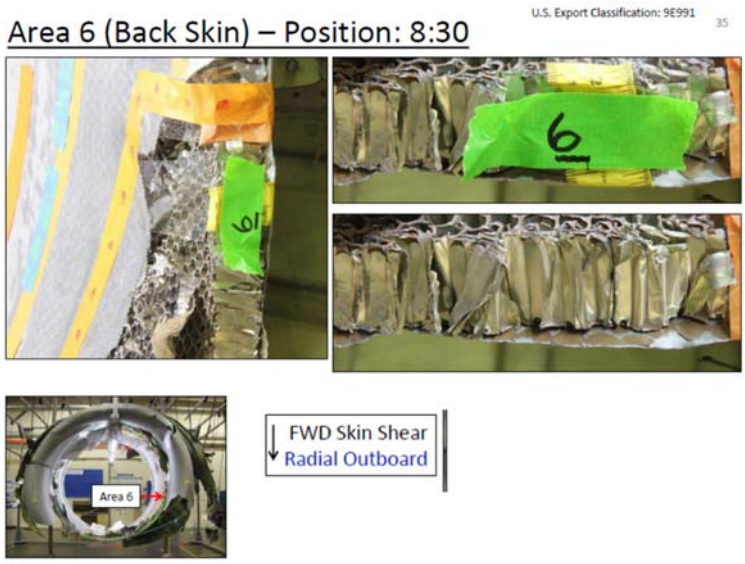

Figure 9-4 Position 08:30

(Reference Oct 2018 Structures Team meeting)

9.3 Phase 2 Inner Barrel Honeycomb Damage

Assessment of inner barrel honeycomb damage within the Phase 2 damage zone from UTAS metallurgical results and visual observations at 7:30 position, Area 56.
A linear cut in the inner barrel honeycomb was noted at the 7:30 position near the forward edge of the containment doubler, see Figure 9-5.
Ti 6-4 particles were found adjacent to the honeycomb cut, see Figure 9-6.
Visual inspection of the cut in the honeycomb showed that the cut was in the outer honeycomb, and that there was partially detached septum and inner honeycomb radially inboard of the cut. The septum and inner honeycomb was rotated into place onto the outer honeycomb with finger pressure. The septum was intact above the cut. A blade fragment could not have cut the outer honeycomb without first cutting through the septum. Therefore, the cut in the honeycomb must have happened after the inner barrel septum separated. This physical evidence indicates the cut in the outer honeycomb at 7:30 was not due to a blade fragment.
This also indicates that the Ti 6-4 material found in the honeycomb at 7:30 position must have come from a source other than a primary blade fragment.which supports that Ti 6-4 on the inner barrel can come from sources other than primary fan blade fragments.

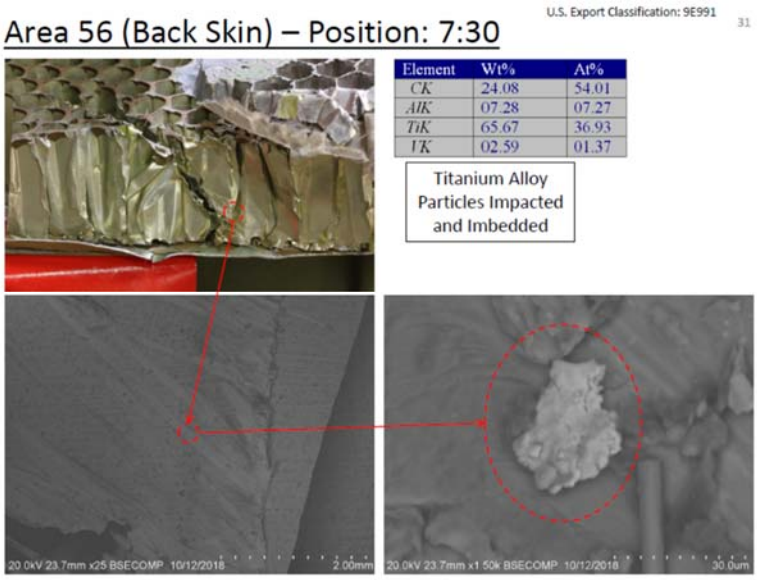

Figure 9-5 Position 07:30

(Reference Oct 2018 Structures Team meeting)

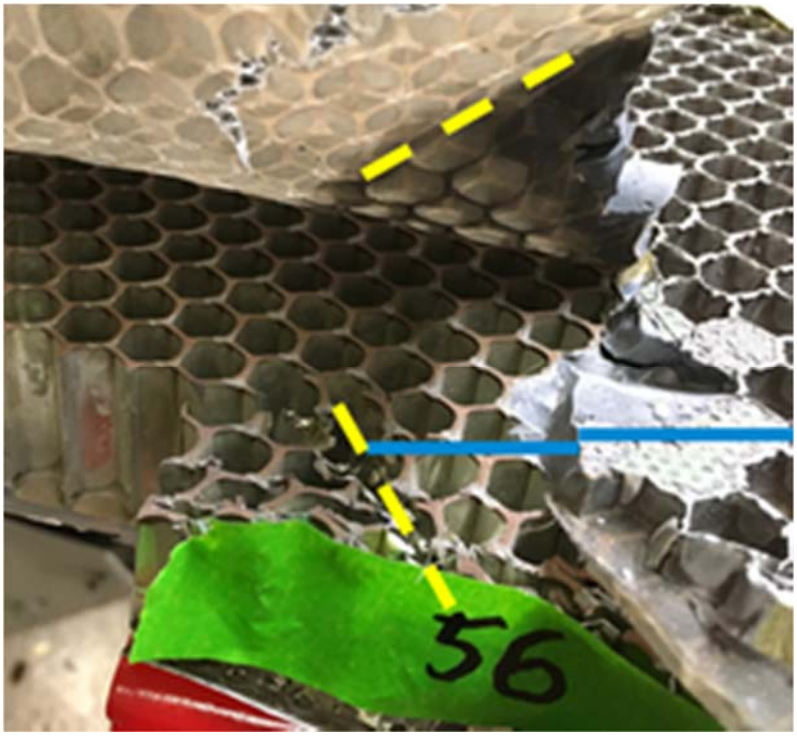

Figure 9-6 Septum above Cut in Honeycomb

(Reference Oct 2018 Structures Team meeting)

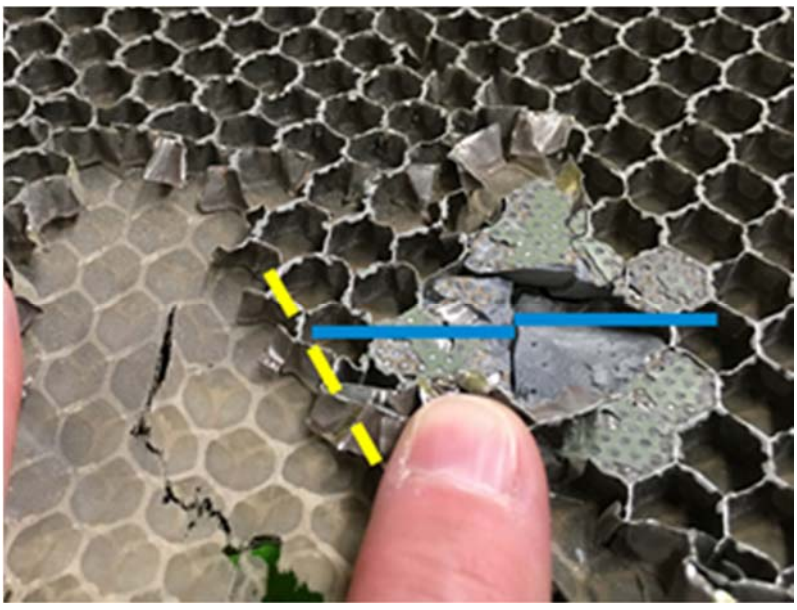

Figure 9-7 Intact Septum Over Cut in Honeycomb

(Reference Oct 2018 Structures Team meeting)

9.4 Other Sources of Titanium Particles

Physical evidence at the 7:30 position of the inner barrel indicated the presence of titanium particles on locations that could not be caused by primary fan blade fragments. This led to consideration of other sources of titanium particles at the inlet separation surface. Two potential sources were identified, small low energy fan blade fragments and material from the Ti 6-4 inlet forward bulkhead.

9.4.1 Small low energy fan blades fragments as source of Titanium particles

Engine fan blade out test experience has shown that many small, low energy fan blade fragments are generated during a fan blade out event. Some of these have forward trajectories. They can also be in motion and exit the fan many revolutions after the blade release. These fragments are small enough and numerous enough that they are not tracked or accounted for in post test summaries.
The total mass of these small fragments can be determined by comparing the total recovered primary fragment masses to the original blade mass. This was done for six CFM56-7 FBO rig tests, and for the 002/4 FBO cert test. The results are shown in Table 3.2.1. On average, 92.9% of the original fan blade mass is recovered. The remaining 7.1%, or approximately 320 grams are made up of small Ti fragments and particles.

Calculated on 6 blades over 5 rig tests (Rig#7 = 2 Blades release) and 1 blade from engine 2/4

Blade (g)	4913
Blade dovetail (g)	353

	Rig#4	Rig#5	Rig#6	Rig#7	Rig#7 (2)	Rig#8	Engine 2/4	
Fragments	3254	730	760	790	790	810	870	
	159	186	210	105	194	153	120	
	139	217	351	408	504	381	33	
	814	150	133	144	197	112	68	
		2810	164	2784	2705	159	84	
			409			196	8	
			2140			2360	3040	
total fragments mass	4366	4093	4167	4231	4390	4171	4223	Average % over 6 bades and 5 rigs tests
% of released blade mass	95,7	89,8	91,4	92,8	96,3	91,5	92,6	92,9

Table 9-1 : Significant blade fragments total mass compared to released blade mass

High speed video data of fan blade out tests captures the presence and behavior of these small fragments. Still images captured from the engine 002/4 cert FBO test show multiple small fragments over a significant duration during the run down.

Figure 9-8 shows a view into the front of the fan approximately 0.13 seconds after blade release. This is immediately after the fan stall has cleared. Multiple, small low energy particles are visible throughout the engine inlet.

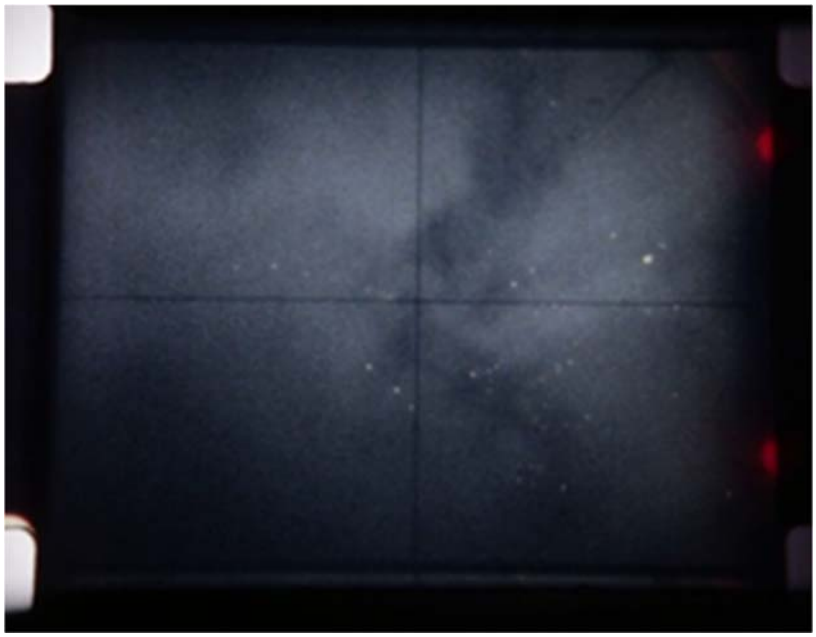

Figure 9-8 High speed video image of engine 002/4 approximately 0.13 seconds after blade release

Figure 9-9 shows a view into the front of the fan approximately 0.6 seconds after blade release. The blue ellipse shows an area of small low energy fragments moving forward in the inlet. Physical evidence from the event hardware also supports the presence of multiple small fragments.

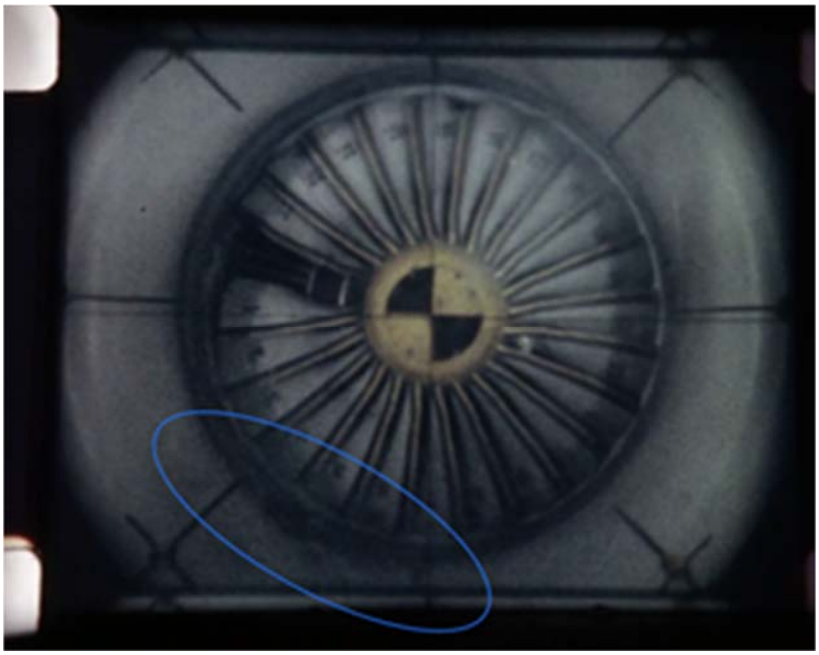

Figure 9-9 High speed video image of engine 002/4 approximately 0.6 seconds after blade release

Figure 9-10 shows marks on the inlet attach ring in the 3:00 to 5:00 region consistent with small, low energy fragments. Physical inspection of these marks showed them to be very light, with no depth. These are consistent with a multitude of small, low energy titanium particles that came forward into the inlet throughout the event, including after the inlet back skin separated. This can account for titanium particles found away from primary fragment locations.

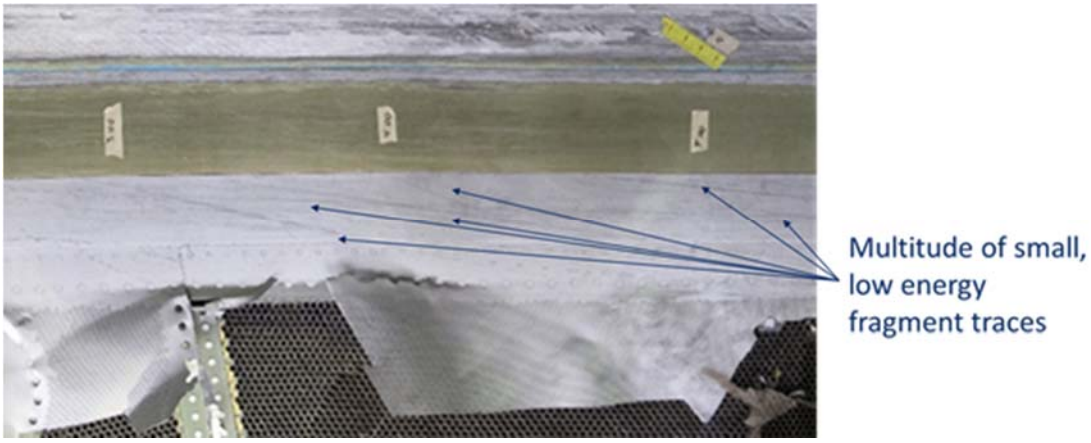

Figure 9-10 Multiple small low energy fragment marks in PHL event inlet

9.4.2 Inlet parts as source of Titanium particles

The other potential source of titanium at the inner barrel separation surface is material from the Ti 6-4 inlet forward bulkhead.

The inlet forward bulkhead is a large Ti 6-4 ring that joins the inner and outer barrel, as shown in Figure 9-11.

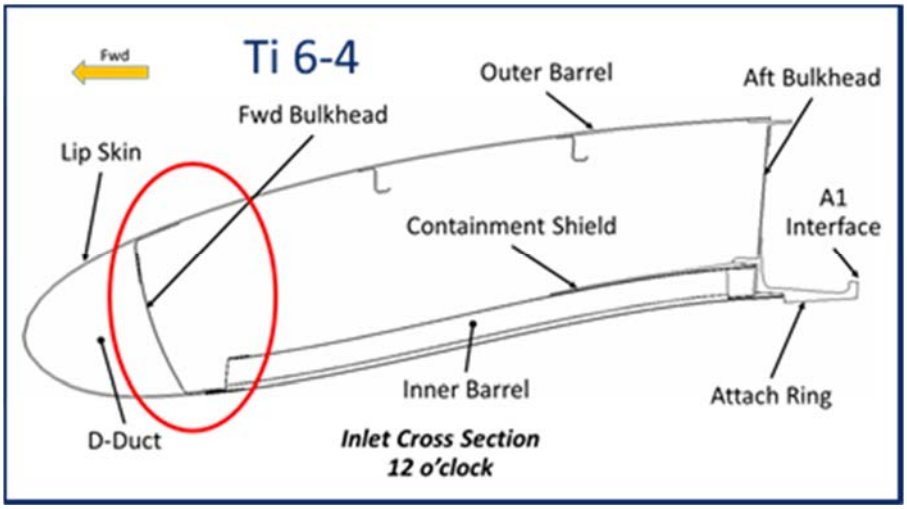

Figure 9-11 Inlet Forward Bulkhead

During the inlet separation, the forward bulkhead was separated from the inner and outer barrel. At the 3:00 location, the forward bulkhead became the aft most surface of the detached part of the inlet. This area of the forward bulkhead was significantly damaged. Physical evidence noted during the party meeting in October, 2018 indicated the forward part of the inlet moved right to left (aft looking forward) across the aft inner barrel fracture surface as it departed. This creates the potential for contact of the exposed Ti 6-4 forward bulkhead with areas of the inner barrel fracture surface, and the presence of additional titanium particles.

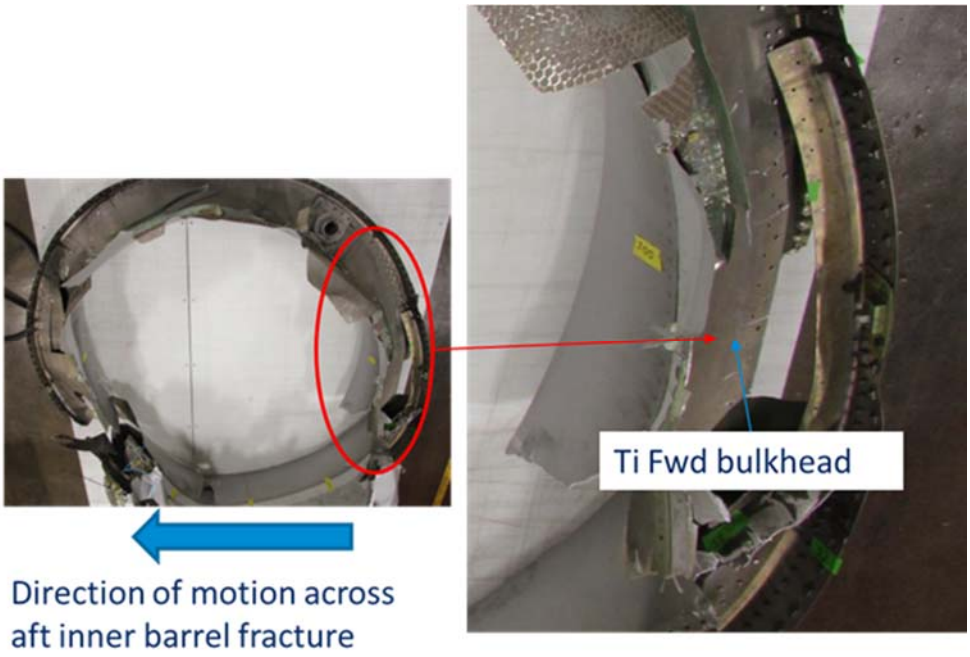

Figure 9-12 Exposure of forward bulkhead and motion across inner barrel

9.5 Phase 2 Perf Skin and Honeycomb Observations

Visual inspection of the inlet inner barrel perf skin and honeycomb condition in the Phase 2 and adjacent areas was conducted during the Party meetings in October, 2018.

It was noted that the majority of the perf skin from 5:00 to 8:30 was still present. Most of the perf skin missing from the aft portion of the inner barrel was still attached to the recovered forward portion of the inlet. Both sides of the perf skin separation were still present as shown in Figure 9-13. This allowed a thorough inspection of the perf skin in this area for evidence of fragment contact or damage. No evidence of fragment trajectory marks or damage consistent with primary fragment contact was present in this area.

In addition to the perf skin condition, the exposed honeycomb was also examined for evidence of fragment damage. See Figure 9-14. The thin inner honeycomb was not crushed and did not show evidence of radial loading that would be expected from a primary fragment.

Both the perf skin and honeycomb conditions in the 5:00 to 8:30 area which includes the Phase 2 area from 7:30 to 8:30 are not consistent with primary fragment presence or damage.

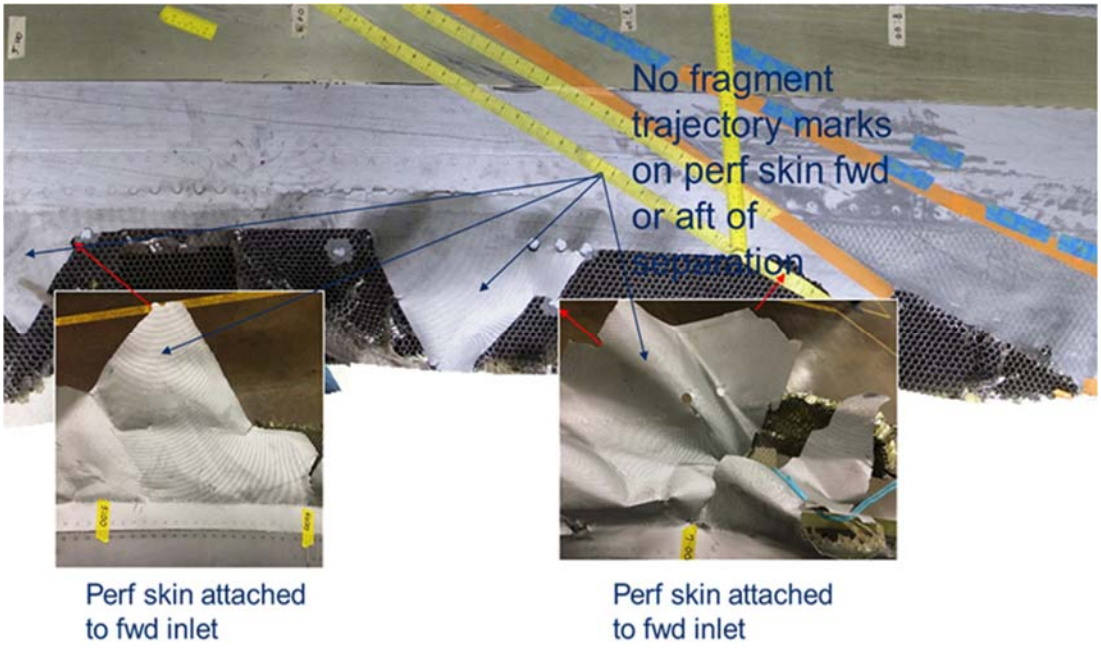

Figure 9-13 Perf skin conditions on both sides of separation in Phase2 area

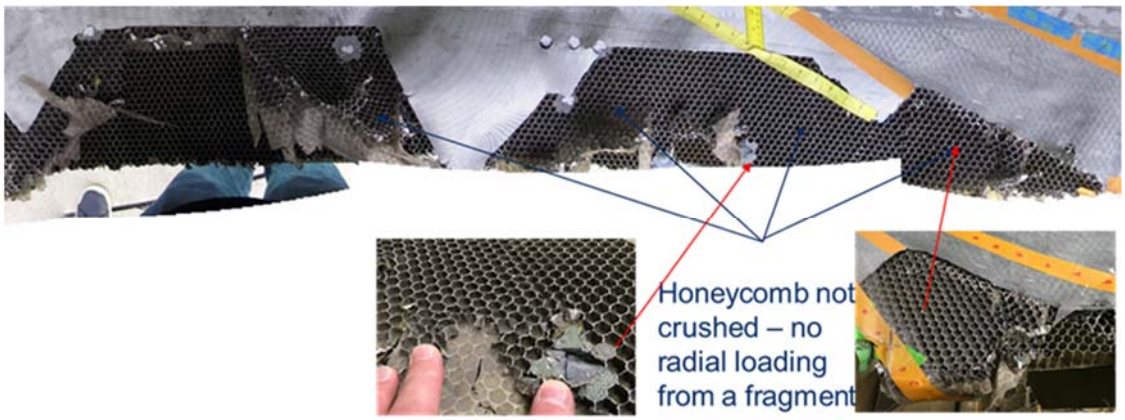

Figure 9-14 Honeycomb condition under perf skin in Phase 2 area

9.6 Assessment of Honeycomb Crushing Adjacent to 9:00 Splice Plate

Additional visual inspections of the inlet inner barrel honeycomb attached to the 9:00 inner barrel splice or beam were also conducted during the Party meetings in October, 2018.

This area is of interest because initial Party assessments suggested that the tip fragment contacted this area and crushed the honeycomb in a circumferential direction as shown in Figure 9-15.

The splice plate at 9:00 is bent back around the outside of the inner barrel. This is believed to be a result of the impact of the separated forward part of the inlet departing in an outward direction (See Figure 9-12). Significant loads were imparted to the splice plate to deform this structural element.

There is a significant amount of inner barrel honeycomb still attached to the deformed splice place. This honeycomb is uniformly crushed in a circumferential direction. Figure 9-16 shows the honeycomb from the inner side of the splice plate. Figure 9-17 shows the honeycomb from the outside of the splice plate. The honeycomb is crushed uniformly through the thickness. This is inconsistent with crushing due to a narrow fragment impact entering from the inner surface. The uniform crushing at the outer back skin surface indicates that the crushing occurred after the honeycomb was separated from the back skin. Also, the honeycomb was

crushed uniformly the entire axial length of the splice plate. This crushed axial width is wider than the expected width of a fragment as shown in Figure 9-15, also indicating this is not consistent with fragment impact.

Figure 9-15 Recovered Honeycomb showing Direction of Crushing

It was also noted that the attached and recovered crushed honeycomb from this area as shown in Figures 9-15, 9-16, and 9-17 consisted of a significant number of honeycomb cells that were crushed to much less than their original thickness. The crushed honeycomb that remained attached to the splice plate included approximately 15 crushed cells. The crushed honeycomb that was separated from the splice plate and recovered as shown in Figure 9-15 includes approximately 12 cells. The original expanded width of these crushed portions of honeycomb can be calculated assuming an uncrushed cell width of 0.375 inch. The attached 15 cells of honeycomb had an original width of 5.6 inches, the separated 12 cells had an original width of 4.5 inches.

This places the original intact face of the honeycomb prior to crushing approximately 5 inches below the edge of the splice plate.

Figure 9-16 Crushed Honeycomb Attached to 9:00 Splice Plate, Inner Side

Figure 9-17 Crushed Honeycomb Attached to 9:00 Splice Plate, Outer Side

This original location of the honeycomb face was then laid out with the inlet and fan case geometry (see Figure 9-18). A red dashed line was constructed from the location at the inlet A1 flange where the tip fragment entered the inlet to the center of the undamaged honeycomb location. This would be the required trajectory for the tip fragment to impact the honeycomb adjacent to the 9:00 splice plate. The angle of the required trajectory would be 40 degrees from circumferential. This is much greater than any physical evidence of the tip trajectory angle. CFM has determined the tip fragment trajectory angle to be 20 degrees per section 4.3). A

trajectory angle of 40 degrees would result in the honeycomb being crushed in a direction 40 degrees from circumferential, which is not consistent with the circumferential direction of crushing observed.
These results all indicate that the honeycomb damage adjacent to the 9:00 splice plate was not due to impact from the tip fragment, and do not support a tip fragment trajectory in this Phase 2 area.

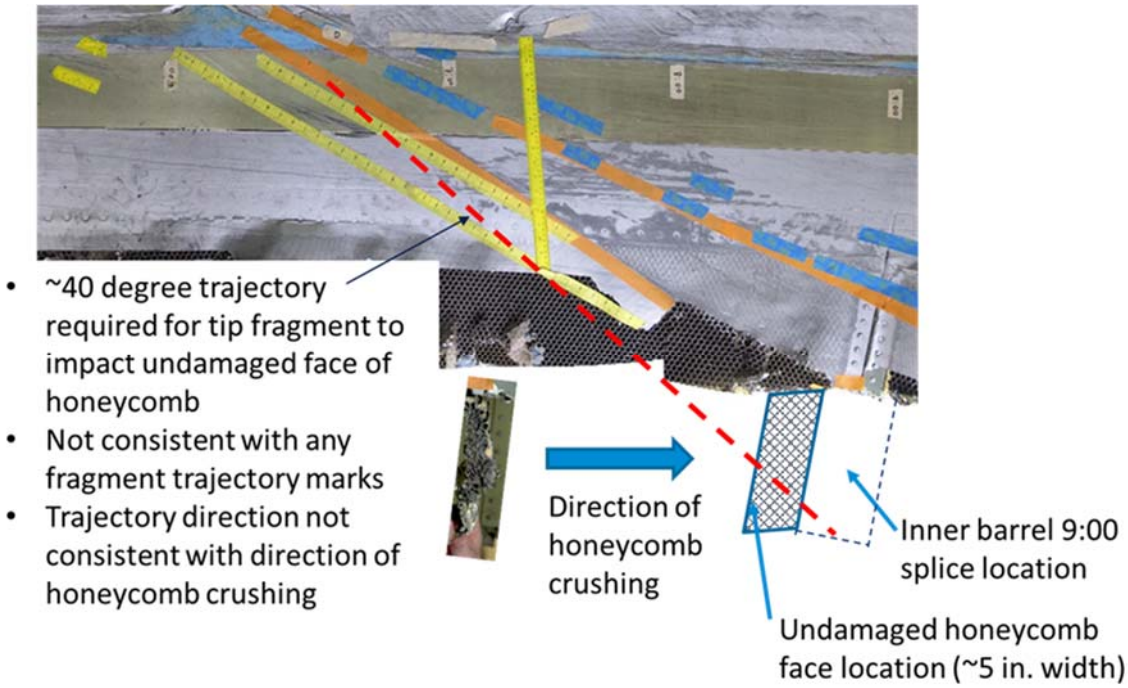

Figure 9-18 Location of Original Undamaged Honeycomb Face and Trajectory Required to Impact It

9.7 Phase 2 Damage Assessment – Conclusion

The evidence from the metallurgical analysis, macro visual condition, fragment trajectory paths, and hardware observations relating to the Phase 2 damage zone extent are combined on Figure 9-19.
There is no evidence of primary fragment marks or trajectories aligned with the Phase 2 damage zone on the perf skin on either the attach ring or D duct side of the inner barrel separation. There is also no evidence of honeycomb crushing from fragment radial loading aligned with the Phase 2 damage. Titanium particles found at 7:30 in the Phase 2 zone cannot be from primary fan blade fragments, and other sources of titanium have been identified. Fragment trajectories observed in the fan case and inlet are not consistent with the Phase 2 damage zone. Therefore, the evidence supports that the Phase 2 back skin damage is not from fan blade fragments.

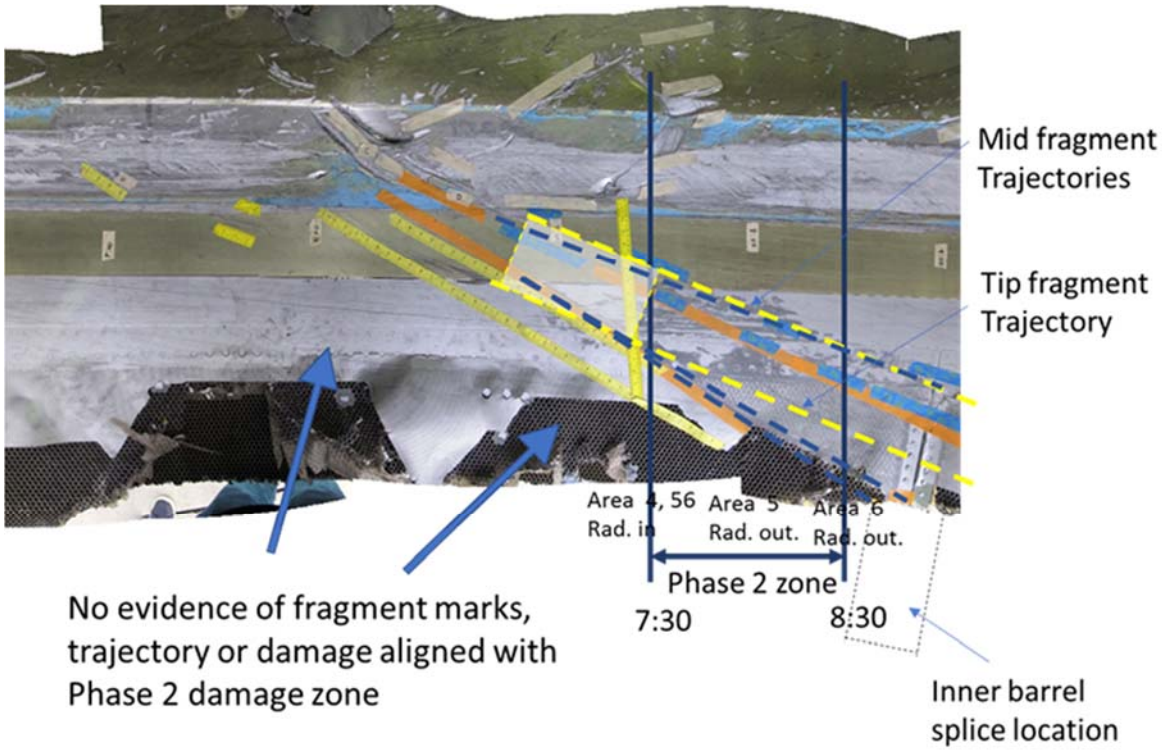

Figure 9-19 Phase 2 Damage assessment

Section 10.0 Phase 3 Inlet Damage Assessment

10.1 Phase 3 Damage Assessment

The Boeing/UTAS definition of the Phase 3 inner barrel backsin damage area at the conclusion of the October, 2018 meeting at UTAS was:
Phase 3 -Damage Supported by Hypothesis of Fragment Damage Progression
Backside skin
Add a circumferential cut in the backside skin, located just forward of the containment doubler forward edge, from 5:00 to 7:30 & 9:00 to 10:30 with no fore-aft width.
Alternating shear lips adjacent to radially out positions added due to hypothesis of 'ripple effects'.

CFM has combined the data from the UTAS metallurgical results with the latest CFM fragment trajectory evaluation, along with additional hardware observations gathered during Structures party examinations of the inlet hardware at UTAS.
There is no evidence of primary fragment marks or trajectories aligned with the Phase 3 from 5:00 to 7:30 damage zone on the perf skin on either the attach ring or D duct side of the inner barrel separation. There is also no evidence of honeycomb crushing from fragment radial loading aligned with the Phase 3 5:00 to 7:30 damage. Fragment trajectories observed in the fan case and inlet are not consistent with the Phase 3 5:00 to 7:30 damage zone. Therefore, the evidence supports that the Phase 3 5:00 to 7:30 back skin damage is not from fan blade fragments.
Metallurgical analysis of back skin failure surfaces in the Phase 3 damage zones 5:00 to 7:30 and 9:00 to 10:30 shows alternating radial shear directions, which are not consistent with fragment penetration.
Therefore, the evidence supports that the Phase 3 (5:00 to 7:30 and 9:00 to 10:30) back skin damage is not from fan blade fragments.

10.2 Inner Barrel Perf Skin Damage Due to Fragments

During the October, 2018 NTSB meeting at UTAS a level of back skin damage due to fan blade fragments was defined to be used in the Boeing progressive damage analysis. The perf skin damage was defined as a rectangular area from 7:00 to 12:00, from the attach ring to 2.0 inches forward of the forward end of the containment doubler. This was based on visual assessment of the perf skin condition after the event.
CFM has assessed the damage to the perf skin due to fan blade fragment considering the perf skin condition, honeycomb damage, fragment trajectories, and other hardware observations as documented in the proceeding sections. The resultant area of perf skin damage due to fragments is shown in Figure 10-1. This results in a trapezoid shaped area starting at 7:30 at the inlet attach ring to 8:45 at the forward end of the containment doubler and ending at 9:30 at the attach ring to 11:30 at the forward end of the containment doubler . This area encompasses all of the primary fan blade trajectories that crossed the perf skin.

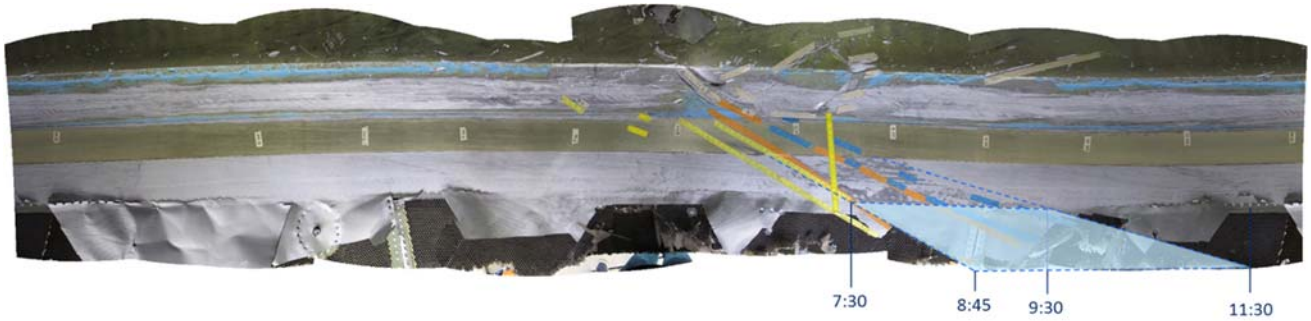

Figure 10-1 Inner Barrel Perf Skin Damage Due to Fragments

Section 11.0 Inlet Damage Assessment - Conclusions

Based on CFM fragment trajectory understanding, UTAS metallurgical findings, and additional hardware observations made during Structures Party meetings, the damage to the inlet inner barrel due to fan blade fragments has been assessed.

The inner barrel back skin damage in the Phase 1 area from 10:30 to 11:30 (30 degrees) is likely due to fan blade fragment penetration. This damage was most likely caused by the tip fragment, with one mid span fragment subsequently passing through the penetration area. This behavior is very similar to the certification and development experience, with the exception of the increased forward travel of the tip fragment

The inner barrel back skin damage in the Phase 1 area from 11:30 to 12:45 is likely not due to fan blade fragment penetration.

The inner barrel back skin damage in the Phase 2 area from 7:30 to 8:30 is likely not due to fan blade fragment penetration.

The inner barrel back skin damage in the Phase 3 area from 5:00 to 7:30 and 9:00 to 10:30 is likely not due to fan blade fragment penetration.

The inner barrel perf skin damage due to fan blade fragments is a trapezoid shaped area starting at 7:30 at the inlet attach ring to 8:45 at the forward end of the containment doubler and ending at 9:30 at the attach ring to 11:30 at the forward end of the containment doubler . This is less than the 7:00 to 12:00 rectangular area defined at the Oct. 2018 meeting at UTAS.